WAGENINGEN UR
For quality of life

Stichting Wageningen Research
Centre for Fisheries Research (CVO)

Investigation of the use of the EK80 CW during acoustic surveys on board Tridens

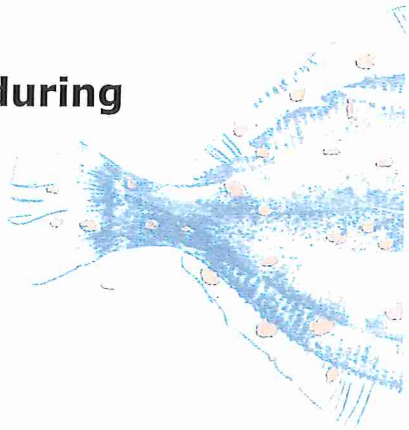

S. Sakinan, B.J.P. Bergès

CVO report: 20.014

June 19th 2020

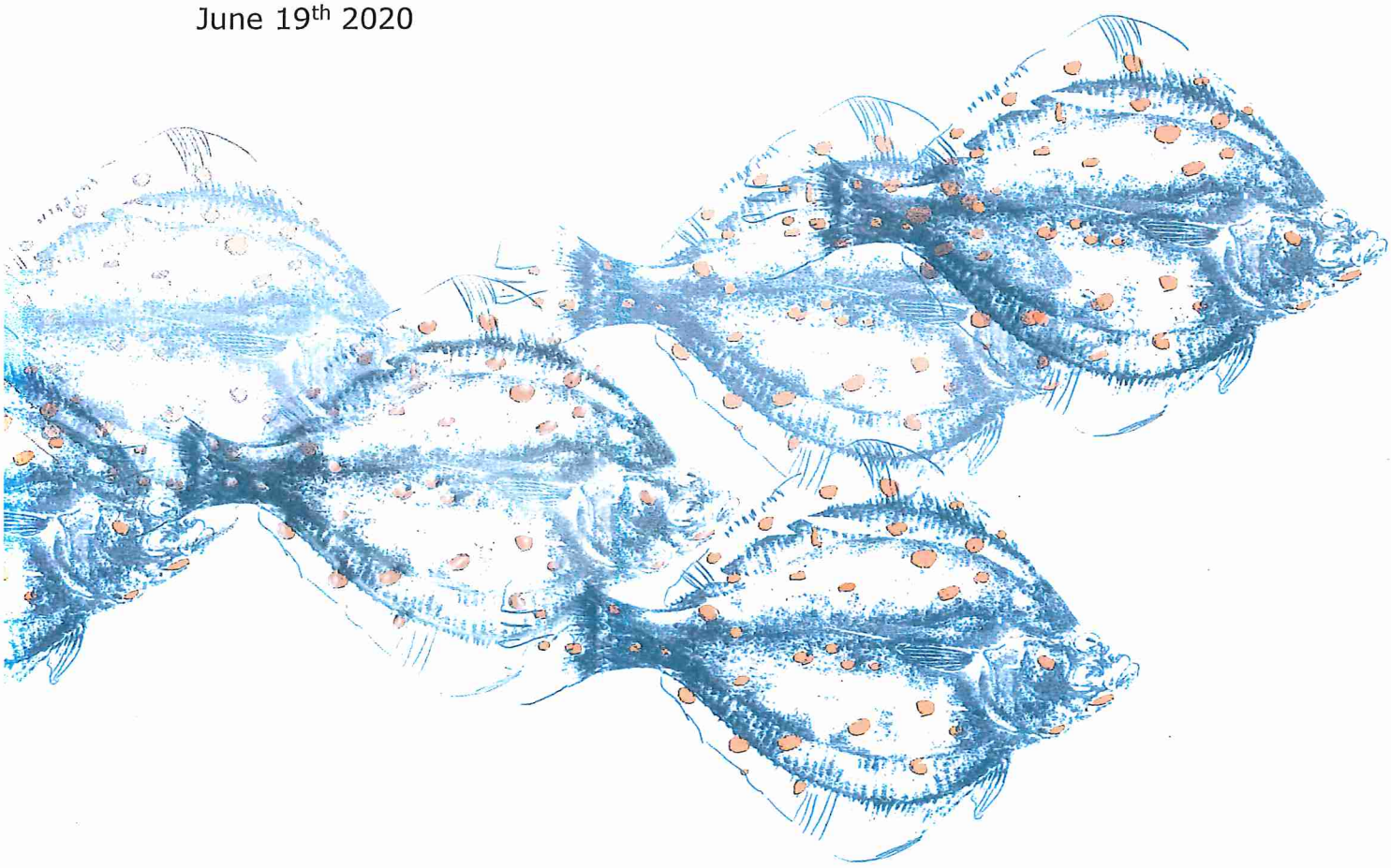

Centrum voor Visserijonderzoek (CVO)

Stichting Wageningen Research
Centre for Fisheries Research (CVO)

Investigation of the use of the EK80 CW during acoustic surveys on board Tridens

S. Sakinan, B.J.P. Bergès

CVO report: 20.014

Commissioned by:
Ministerie van LNV
Directie SKI
Postbus 20401
2500 EK DEN HAAG

Project number: 4311300061
BAS code: KB-24-005-019

Publication date: 19th of June, 2020

Stichting Wageningen Research
Centre for Fisheries Research (CVO)
P.O. Box 68
1970 AB IJmuiden
Phone. +31 (0)317-487418

Visitor address:
Haringkade 1
1976 CP IJmuiden

This research is part of the statutory task programme "fisheries research" and funded by the Dutch Ministry of Agriculture, Nature and Food Quality.

DOI: https://doi.org/10.18174/524591

CVO rapport ENG V09

Table of Contents

Summary

Fisheries acoustic surveys are routinely conducted around the world, and particularly within the ICES community. For nearly 20 years, the Simrad EK60 system has been the most commonly used echosounder equipment, and it is now being superseded by the Simrad EK80 system (CW mode). The comparison of the two systems and the impact of the transition from one system to the next for routine acoustic surveys has been investigated by several institutes. This report specifically investigates the use of the EK80 CW on board the Dutch Research Vessel (RV) Tridens II.

RV Tridens II is routinely used by Wageningen Marine Research for conducting acoustic surveys. Currently, while the EK80 system is also available on board, the EK60 is used for survey recordings. In order to bring a transition from the EK60 to the EK80 CW, this study investigated:

1. the consistency in calibration results for the EK80 CW since 2015. This is done by generating time series plots of historical EK80 CW calibration data collected on RV Tridens II.
2. the consistency between the EK60 and the EK80 CW with data collected ping to ping using a multiplexer during the herring acoustic surveys (HERAS) in 2017 and 2018.

The EK60/EK80 CW results are also put in light of findings of another published study (Macaulay et al. 2018) based on data collected on RV Tridens II in 2016 during the blue whiting acoustic (IBWSS) survey.

Calibration and EK60/EK80 CW results from HERAS 2018 reveal large discrepancies with the EK80 CW 38 kHz channel originating from July 2017. The EK60/EK80 CW results from HERAS 2018 also show smaller discrepancies for the 18 kHz channel, due to different areas of the acoustic ring down below the transducer and noise interferences of the EK80 CW. Nevertheless, the analysis of other frequency channels for both HERAS 2017 and 2018 data show a good agreement between the systems. In addition, the analysis of 18 kHz and 38 kHz channels for HERAS 2017 exemplify good consistency between the EK60 and the EK80 CW, suggesting an electrical problem is causing the discrepancies observed during HERAS 2018. Though the issue with the 18 kHz and 38 kHz channels on board RV Tridens II needs to be tackled prior to using the EK80 CW for routine surveys, this study together with previous studies suggest that results from the EK80 CW are comparable to those of the EK60. It is therefore recommended to switch to using the EK80 CW for routine acoustic surveys onboard RV Tridens II once the issue with the equipment malfunctioning is resolved.

1 Introduction

Fisheries acoustic surveys are routinely conducted around the world, and particularly within the ICES community. Following pre-defined transects, these surveys make use of downward active acoustic systems (i.e. so called scientific echosounders) to estimate abundance and distribution of marine species (Mehl et al. 2018; Dalen and Nakken 1983; Simmonds and MacLennan 2005). This type of survey is often used to derive abundance indices for a specific stock which are subsequently used in stock assessments. An example is shown in Figure 1 for the Herring Acoustic Survey (HERAS; North Sea herring) and the International Blue Whiting Spawning Stock Survey (IBWSS; blue whiting west of Ireland) surveys. These surveys follow the guidelines in the dedicated manuals issued by ICES (ICES 2015). An important characteristic for the survey index is consistency in tracking cohort through the years in order to track a given stock with limited influence from change in methodology. When planning the survey, it is a key priority to introduce as little bias as possible and minimize the changes in specific survey protocols (transect design, survey coverage etc) as they are highly influential for the resulting survey index. However, a potential further source of bias is the echosounder itself. The inter annual change in sensitivity of the echosounder is tackled through dedicated calibration. Because echosounder calibration is a very well defined and controlled exercise (Demer et al. 2015; K. G. Foote et al. 1987), it is possible to track any doubtful change in the echosounder response by comparing historical calibration results. However, some electrical problems are not always revealed during calibration. Also, any change in echosounder model on the different Research Vessels (RV) should be documented and investigated thoroughly to assess and minimize the effect on the acoustic recordings.

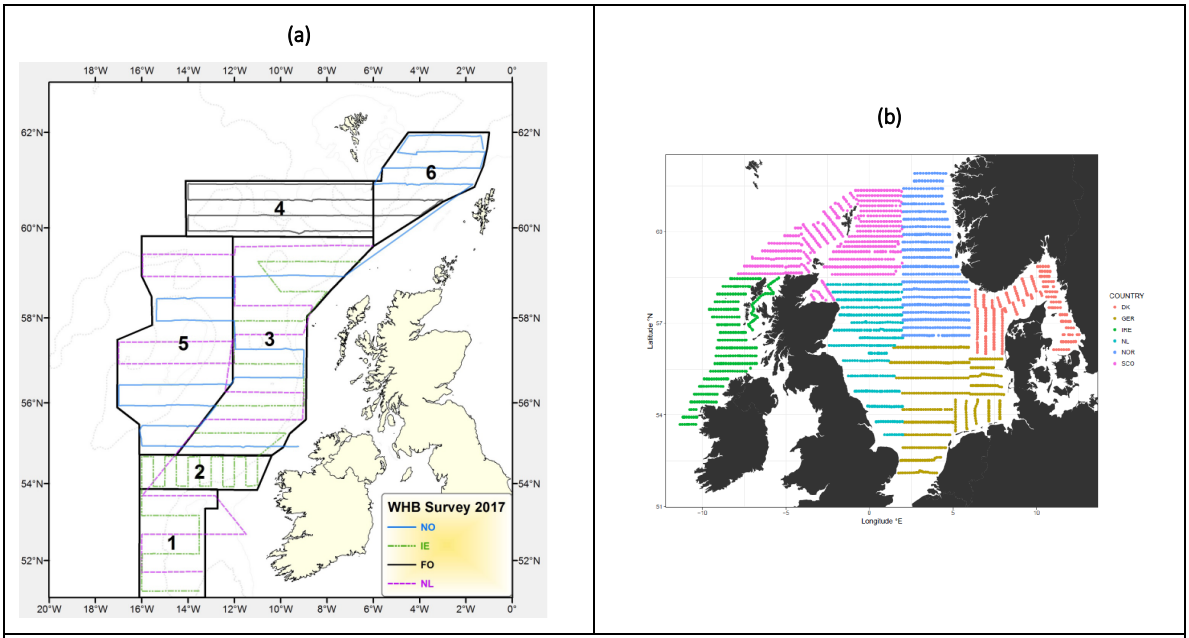

Figure 1: *Survey coverage (i.e. transects) for the International Blue Whiting Spawning Stock Survey (IBWSS) (a) and Herring Acoustic Survey (HERAS) (b) in 2018. The different colours represent the countries involved in each survey. Both graphs are extracted from* (ICES 2018b).

For example, in the 2000s, a transition from the Simrad EK500 to the EK60 occurred at various institutes. This transition was necessary as the EK500 system was no longer supported by Simrad. Both systems were narrowband but the EK60 presented several technological advancements that allowed for example more swift calibration trials. These changes motivated several studies and workshops at the time (Jech et al. 2005; NOAA 2004) and the EK60 system was subsequently gradually introduced by marine institutes for regular acoustic surveys.

The last nearly 2 decades, the Simrad EK60 system (narrowband) has been the most commonly used equipment and it is now being superseded by the Simrad EK80 system ran in Continuous Wave (CW) mode. Though the EK60 is currently used by several institutes, it is no longer officially supported by Simrad and the transition to the EK80 CW is necessary in the near future. The EK80 CW is to differentiate with the EK80 running in Frequency Modulated (FM) mode: the EK80 CW is transmitting narrowband signals while the EK80 FM is transmitting broadband signals, which require much more storage space and provide essentially different data. The future use of FM data requires extensive investigations before it can be used for the analysis of fish abundances. This study deals with the collection of EK80 CW data.

The comparison between the EK60 and the EK80 CW is topical and has been investigated by several institutes (ICES 2017, 2018a; Macaulay et al. 2018; Demer et al. 2017; Sakinan et al. 2018). Though results show that the two systems are nearly equivalent, it is important to assess this transition for each RV, in different conditions if possible. To that purpose, this study investigates the use of the EK80 CW on board the Dutch RV Tridens II (routinely used by Wageningen Marine Research (WMR) for conducting acoustic surveys). In addition, one must ensure that the installed EK80 CW setup is robust through the years. More specifically, this report will present results on:

1. The consistency in calibration results for the EK80 CW since 2015. This is done by generating time series plots of historical EK80 CW calibration data collected on RV Tridens II.
2. the consistency between the EK60 and the EK80 CW with data collected ping to ping using a multiplexer during HERAS in 2017 and 2018.

On board RV Tridens II, the following frequency channels are available for both the EK60 and EK80 CW systems: 18 kHz, 38 kHz, 70 kHz, 120 kHz, 200 kHz and 333 kHz. In this study, the 333 kHz channel will not be considered as it has been malfunctioning in the recent years and is also the least valuable channel. This is because of its limited depth penetration capabilities due to higher acoustic absorption for higher frequencies. In addition, it is important to note that there are frequency channels that are more important than others. The 38 kHz channel is central for acoustic surveys because the abundance estimation is solely based on the acoustic scattering at this frequency. The other frequencies are less valuable and most often only used during the scrutiny process, for example to differentiate marine species based on their acoustic fingerprint (Korneliussen et al. 2016)

2 EK80 CW Calibration

Scientific echosounders are designed to be extremely sensitive and Simrad provides details about the performance of their systems when delivered. Still it remains essential to assess the accuracy and precision of the system before any survey through a calibration trial. After this process, the echosounder should provide absolute acoustic measurements (required for abundance estimation) and therefore cross comparison between different vessels in the same sampling area is possible (e.g. HERAS survey, Figure 1).

On RV's, the calibration is performed at sea using standard calibration spheres (Demer et al. 2015; K. G. Foote et al. 1987). The target strength (TS) from such targets are well established theoretically and the comparison with the measurements from the echosounder provides the compensation needed for the system to provide absolute acoustic scattering measurements. The quality of the data collected during the calibration trial can vary for example with weather conditions, the quality of the sphere, and the quality of the rigging (MacLennan 1981; Simmonds and MacLennan 2005; Kenneth G. Foote 1982; Hobæk and Nesse 2006). It is therefore paramount to have numerous calibration trials together with a record of the historical results in order to track the performance of the system. A critical problem may not be immediately obvious from year to year, therefore having time series information and visualisation is important for timely detection of the problems.

In this project, a data management strategy together with the relevant R codes was developed in order to track the specificities and results of the different calibration trials performed on board RV Tridens II. As shown in Figure 2, a typical fisheries acoustic survey consist of data collected during the calibration trial and the survey itself. The analysis of these data allow the acoustic specialist to produce outputs for the survey (e.g. in the form of acoustic abundance per nautical mile). Within WMR, all data are being stored in internally together with all acoustic survey data (raw data, calibration results, survey results). However, because different surveys (and different survey periods) are conducted by different scientists, it is often difficult to efficiently track all the results across the years, especially regarding calibration. To that purpose, all EK80 CW calibration results to date in the form of *.xml files (direct output of the calibration procedure) were collected and gathered in a common location. Then, code was developed to automatically read these *.xml files and generate an overview of all the calibration results performed on RV Tridens II. In this section, a summary of the results will be presented. The full report generated at the time of writing (January 2019) is given in Annex I.

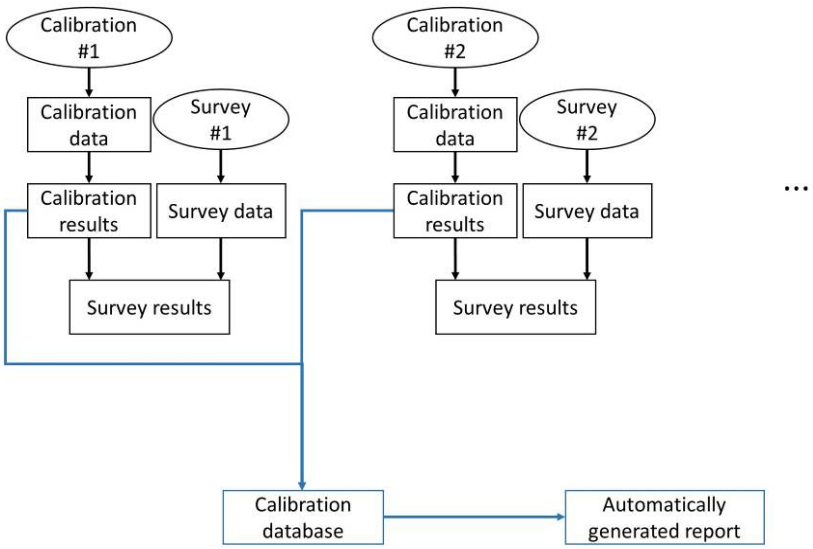

Figure 2: *Schematic of data collected during survey and calibration trials. The blue lines represent what was developed within this project (calibration database and automatic report generation).*

2.1 Data collection

During a calibration trial on board RV Tridens II, calibrations spheres are first lowered in the water below the transducer (Demer et al. 2015; K. G. Foote et al. 1987). The spheres are attached to 4 winches on the vessel deck. Each winch is automatically controlled, allowing the operator to control the position of the sphere in the water. The sphere is then positioned below a given transducer. RV Tridens II has six transducers: 18 kHz, 38 kHz, 70 kHz, 120 kHz, 200 kHz and 333 kHz. While a given transducer is being calibrated, the other ones are set to passive. The echo trace from calibration spheres is distinct, as shown in Figure 3(a). Once the sphere is stable, the operator starts the EK80 CW calibration software (Figure 3(b)). This allows the operator to monitor the state of the recording (e.g. coverage, data quality). Raw data are recorded through the whole process.

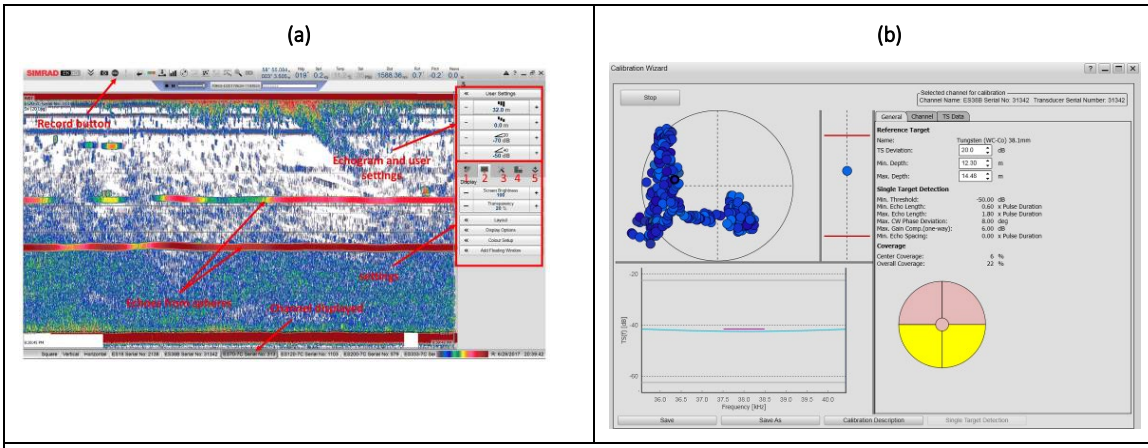

Figure 3: *Screenshots of the EK80 CW software during a calibration trial. (a) Main echogram display during calibration; (b) Calibration GUI of the EK80 software.*

Typical calibration spheres consist of: 63 mm diameter copper, 38.1 mm diameter tungsten carbide, 25 diameter mm tungsten carbide, 22 diameter mm tungsten carbide. Specific spheres such as the 63 mm diameter copper are optimized for specific channels (18 kHz) and are not useable for other channels (e.g. 333 kHz). For this reason, the operator can change the type of sphere in the water depending on which EK80 CW channel is needed to be calibrated.
Data from the calibration trials gathered and used in this study for the EK80 CW are:

- HERAS, June 2018, Scapa Flow - 18,38,70,120,200 kHz.
- IBWSS, March 2018, Bantry Bay - 38,70,120,200 kHz.
- HERAS, June 27, 2017, Scapa Flow - 18,38,70,120,200,333 kHz.
- IBWSS, March 2017, Lands' End - 18,38 kHz.
- HERAS, June 2016, Scapa Flow - 18,38 kHz.
- IBWSS, March-April 2016, Little loch broom - 18,38,70,120 kHz.
- Out of survey calibration, February 2016, Norway - 38,70,120,333 kHz.

Several bugs with the calibration software of the EK80 CW were previously found and reported by (Sakinan et al. 2018). Calibration results were thoroughly checked in this study.

2.2 Results and discussion

Plots and tables generated using an automatic report generation (R code) are presented in Annex I. This includes summary tables and plots for each calibration trial (Table I.1 to I.7 and Figure I.1 to I.7) together with plots of the calibration results (TS offset and gains) in time for both the EK60 and the EK80 CW (Figure I.8 and I.9 respectively).

It is important to note that because the EK80 CW is – at the time of writing - not yet the system used for data collection during surveys, it is behind the EK60 (system of choice for data collection) in term of priority during calibration trials. As a result, overall, the number of data points for the EK80 CW is less than for the EK60. In term of measurements across the frequency channels, the priority is always the 38 kHz channels, the one that is most commonly used for survey echo integration (i.e. abundance estimation). The calibration of other frequency channels is important for the scrutiny process (differentiating fish species based on their finger prints) but are only calibrated if time allows. The calibration for the EK60 was found to be valid while for the EK80 CW, discrepancies were found for the 38 kHz channel. This is exemplified further in this section.

TS gain overtime for the 38 kHz channel for the EK60 and EK80 CW are replicated in Figure 4 and Figure 5. On both graphs, the uncertainty of each measurement is shown with error bars: the Root Mean Square (RMS) error margin. On a normal practice, a decision for a good calibration is made by looking at this RMS error in the Target Strength (TS) gain. If this RMS error is smaller than 0.4 dB then calibration is deemed to be valid. However, critical problems with transducers or the transceivers are not necessarily revealed by large RMS errors.

In Figure 4, it can be observed that for the EK60, the gain is stable over time with a variation of 0.2 dB. In addition, the uncertainty across the different measurements is minor and below the threshold of 0.4 dB. Figure 4 exemplifies the robustness of the EK60 system on board RV Tridens II since 2015.

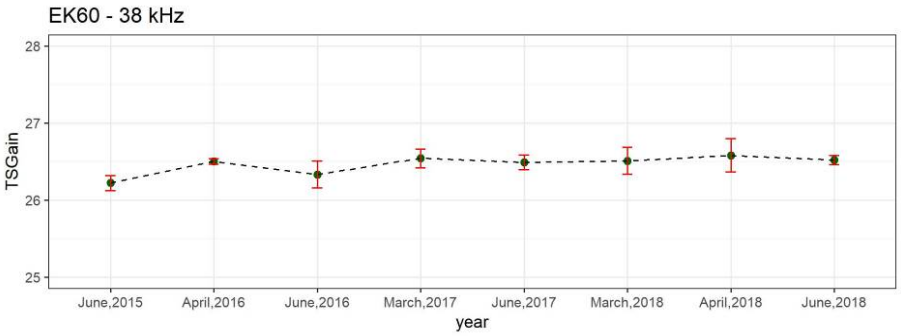

Figure 4: *Calibration tests for the 38 kHz system. Red whiskers show the RMS error margins for the test results.*

Figure 5 shows the TS gain over time for the EK80 CW at 38 kHz. First, the low RMS error across all measurements demonstrates a good accuracy of the system overall. However, a sharp drop (2 dB) can be observed between June 2017 and March 2018. Though change in transceiver sensitivity and therefore gain are expected over time, the variation over a period of a year rarely exceed 0.1 dB. This is exemplified in Figure 4 for the EK60 with a TS gain that is stable around 26.5 dB. The TS gain is specific to both the transducer and the transceiver and differences in gain between EK60 and EK80 CW is expected. However, the drop of 2 dB in the EK80 CW time series reveals a malfunctioning occurring between June 2017 and March 2018. In addition, because this drop in TS gain is not observed for the EK60, it can be inferred that the transducer is functioning well. The issue likely lies with either the EK80 CW transceiver itself or its connection to the transducer.

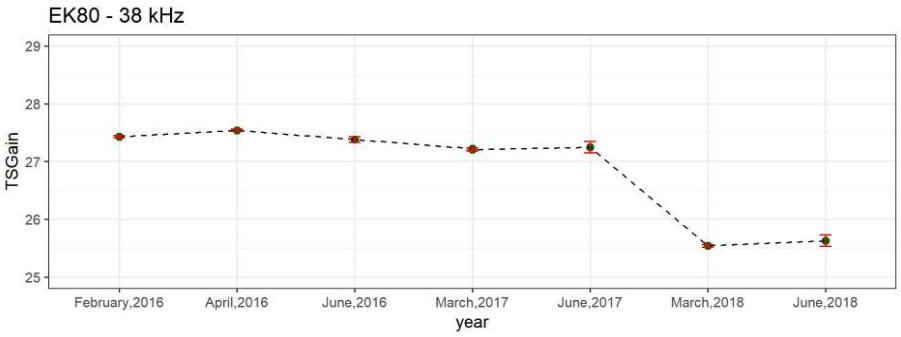

Figure 5: *Calibration tests for the 38 kHz system. Red whiskers show the RMS error margins for the test results.*

3 EK80 CW/EK60 comparison

Because the EK80 CW will supersede the EK60 for data collection during ICES acoustic surveys (HERAS, IBWSS) in the next years, it is important to investigate the impact of such a change on board RV Tridens II. This section will also investigate a discrepancy in the EK80 CW calibration highlighted in Section 2. This consists of an unusually large drop in TS gain between June 2017 and March 2018.

In the context of this study, two earlier comparisons of EK60 and EK80 CW performances need to be highlighted. Sakinan et al. (Sakinan et al. 2018) investigated the functioning of echosounders on different commercial Pelagic trawler Fishing Vessels (FV) running a mixture of EK80 CW and EK60 systems. As a baseline for this study, data from RV Tridens II was used. More specifically, partial ping to ping data collected in July 2017 was used. Good correlation between the EK60 and the EK80 CW was found (see Figure 6). The present study will analyse the same data set, expanded with data collected in 2017 and 2018.

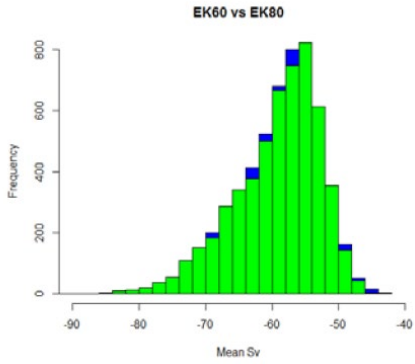

Figure 6: *Comparison of frequency distribution of echo-levels (S_v) for the 38 kHz channel between EK60 (blue bars) and EK80 (green bars). Extracted from Sakinan et al. (2018).*

The study by Macaulay et al. (Macaulay et al. 2018) investigated in depth the performances of the EK60 and the EK80 CW by using ping to ping data collected in 2016 by RV Tridens II and RV G.O. SARS (Norway) during the IBWSS survey. This study shows that the magnitude of variability between the two systems is smaller than the stochastic variation expected from echosounders. Despite their results being conclusive for RV Tridens II, the data show greater variability compared to RV G.O. SARS. This could be due to the use of different data sets (North Sea for RV G.O. SARS, West of Ireland for RV Tridens II), leading to each collected data having specific characteristics (depth, aggregation type, season). Overall, Macaulay et al. (2018) shows that the change from EK60 to EK80 CW is satisfactory. The results show differences that are generally less than other sources of bias and error in acoustic surveys and stock assessment processes (Macaulay et al. 2018). This also includes RV Tridens II in the context of the IBWSS survey. The present study complements Macaulay et al. (2018) for RV Tridens II through the following:

- Comparison between EK60 and EK80 CW during the HERAS survey. There are two main differences compared to RV Tridens II data used in (Macaulay et al. 2018):
    - Data used by Macaulay et al. (2018) (IBWSS) were collected under different environmental conditions compared to the area surveyed during the HERAS survey (e.g. depth, temperature and aggregation characteristics of the target fish).
    - Data used by Macaulay et al. (2018) (IBWSS) have a ping rate of 2 seconds due to the large operating depth (~750 m). During the HERAS survey, the operating depth is usually below 150 m and the standard ping rate is 0.6 seconds.

- In Macaulay et al. (2018), each frequency channel was tested individually, i.e. while one frequency channel was active, the other channels were set as passive. For the data used here, all frequencies were multiplexed at the same time. Therefore, the same aggregations were observed on the different frequency channels. The latter is the standard way of collecting data during routine acoustic surveys.
- In Macaulay et al. (2018), backscatter from the seabed was also included. In the present study the focus is constrained to the water column (i.e. excluding the seabed).

3.1 Data collection

The analysis in this section was carried out with data collected during the HERAS in 2017 and 2018. The data consists of EK80 CW and EK60 collected ping to ping using a multiplexer. The multiplexer works as a switch between the transceivers and the acoustic transducers. In short, it is switching the coupling of specific transducers with either the EK60 or EK80 CW systems. Data were collected using simultaneous pinging at the following frequencies: 18 kHz, 38 kHz, 70 kHz, 120 kHz, 200 kHz. For both the 2017 and 2018 surveys, respectively 241 km and 296 km of ping to ping data were collected and analysed. The HERAS 2017 data set mainly consists of recordings between transects while the HERAS 2018 data set is a combination of recordings during survey tracks and around fishing operations. The extent to which ping to ping data could be collected along survey transects was dependent upon not disturbing routine survey tasks, the use of the multiplexer adding complexity in the data collection. The corresponding transects are shown in Figure 7. In contrast, RV Tridens II data presented in (Macaulay et al. 2018) were collected for each frequency individually with 116 km of data at most (Macaulay et al. 2018, Table 2). Also, RV Tridens II data used in (Macaulay et al. 2018) at 38 kHz were used to check the consistency of the analysis presented in this report.

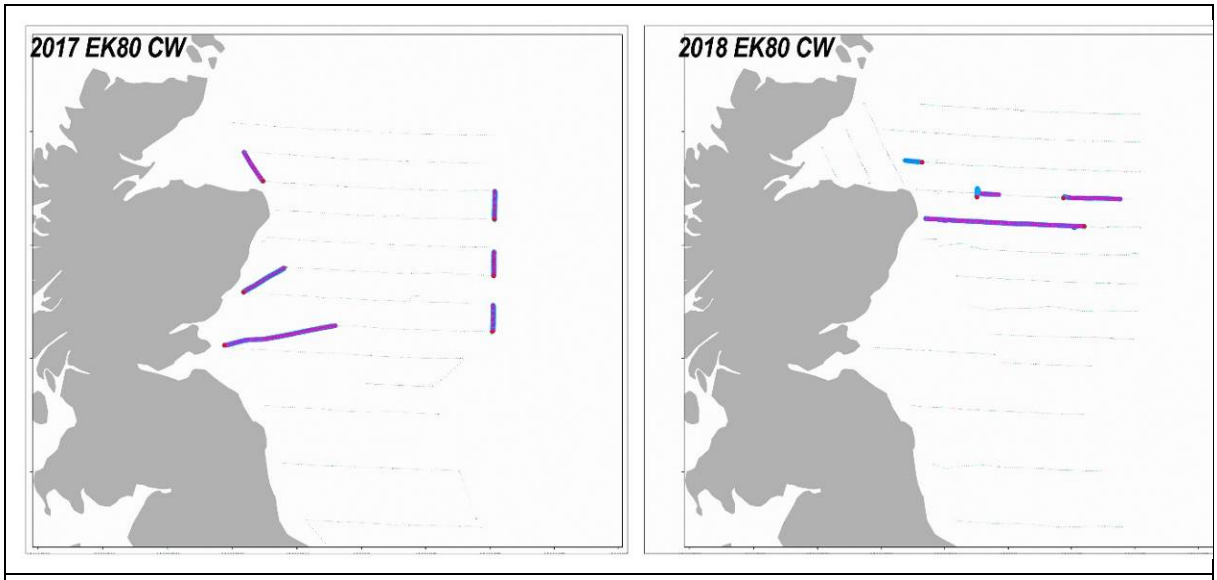

Figure 7: *Ping to ping data used for this analysis: HERAS 2017 (left graph, 241 km), HERAS 2018 (right graph, 296 km in total). The grey lines are the survey transects followed during the respective surveys. The highlighted transect sections are those where EK60/EK80 CW ping to ping data was collected.*

Specific noise problems were experienced with the EK80 CW at 38 kHz during HERAS 2018. This is likely to cause the discrepancy observed from the calibration data and highlighted in Section 2 (Figure 5). In order to investigate this noise issue further, the entire set of HERAS 2017 EK80 CW data is scrutinized for the appearance of noise patterns. This includes analysis of data collected using the EK80 CW without the multiplexer (e.g. data collected during fishing operations). The source of this noise will be investigated and discussed in the next sections. In addition, compared to the HERAS 2017 data, the HERAS 2018 data are

overall noisier due to interference of other acoustic equipment such as omnidirectional sonar when on in the trawling regions.

3.2 Material and methods

Using the ping to ping data described in Section 3.1, the acoustic postprocessing is performed using the Echoview software (version 9)[1]. The analysis presented here includes two processes:

- Ping to ping stochasticity study. Data collected by echosounders are inherently stochastic and it is important to investigate the extent of the ping to ping variability. This is done by studying the ping to ping correlation of EK60 records and this works as a baseline for the EK60/EK80 CW comparison.
- Ping to ping comparison between EK60 and EK80 CW.

Both analyses are carried out on each data set separately (HERAS 2017 and 2018) because of the differences in data collection setup. For a given set of data the following post-processing workflow is used:

- Time alignment between EK60 and EK80 CW records. This is to ensure that all compared pings at all frequencies match relevant time stamps.
- Creation of the bottom line using a combined echogram. The combined echogram is a result of all channels. The bottom line was defined for both the EK60 and the EK80 CW with the maximum acoustic scattering value. After generating the bottom line, manual scrutiny was carried out.
- A surface filter is used, using an upper bound limit of 20m from the surface.
- There is unavoidable natural variability in the data that are collected and this can be assessed by comparing consecutive pings for the same equipment. This was done using the EK60 data. For this EK60 ping to ping variability comparison, two EK60 data subsets are generated by grouping all even and all odd EK60 pings. These are then treated as two separate data sets (EK60_even and EK60_odd). The correlation between these two subsets provides insight into the natural variability to be expected between the EK60 and the EK80 CW.
- Data resolution is reduced to 102 seconds (horizontal) and 5 m (vertical) bins. This is consistent with (Macaulay et al. 2018). This coarse gridding is then exported as csv files. The acoustic quantity that is exported from the grid is Sa which is the integration of Sv across depth bins and averaged over pings (Maclennan, Fernandes, and Dalen 2002). The quantity Sv is the Volume backscattering coefficient (acoustic scattering corrected for propagation losses and gain).The resulting export is a grid of Sa value for each grid point along depth and distance (nmi).
- After exporting data to csv files, extreme outliers caused by noise spikes are removed (using > 0.999 and < 0.001 quantiles).
- For numerical comparison T-test and linear regression is performed. Corresponding parameters are extracted and presented on each resulting plot:
    a. Slope: The regression slope
    b. RMS: Root Mean Square error of the regression
    c. T-value: Result of the t-test showing the magnitude of the difference relative to the variation. A value closer to zero means that the difference is smaller (either from positive or negative direction).
    d. P-value: Result of the t-test showing the significance of the difference between pairs. A P-value smaller than 0.05 means that the difference is significant. A P-value greater than 0.05 exemplifies differences that are not significant.
    e. **Δ** Sa : Median of the differences in area backscattering strength (Maclennan, Fernandes, and Dalen 2002).
    f. R^2 : Correlation coefficient of the linear regression.

[1] Echoview Software Pty Ltd, Hobart, Tasmania, https://www.echoview.com/

The post-processing employed here has a few differences compared to the method used by Macaulay et al. (Macaulay et al. 2018) on the RV Tridens II data. Of relevance are the following points:

- During the IBWSS 2016 data collection and used by Macaulay et al. (2018), only one frequency channel was active while other channels were set as passive. In the study presented here, data are collected while pinging simultaneously across all the frequency channels.
- (Macaulay et al. 2018) used a total of 54 km of recordings for the EK60 variability test. These data do not overlap with the data used for the EK60/EK80 CW comparison. Here, the same datasets are used for both EK60 variability study and EK60/EK80 CW comparison.
- (Macaulay et al. 2018) used a ping rate of 4-6 seconds. This corresponds to an effective switch between EK60 and EK80 every 2-3 seconds. The ping rate was reduced to 1.2 second during HERAS 2017 and 0.6 – 1.2 seconds during HERAS 2018. This corresponds to an effective switch between EK60 and EK80 every 0.3-0.6. The difference is mainly due to the large depth during the IBWSS survey (~750 m as opposed to ~150 m during HERAS)
- (Macaulay et al. 2018) included the sea bottom in the analysis (when present). In the present study, the sea bottom was excluded by using the bottom detection function of the EK80/60 software.

3.3 Results and discussion

3.3.1 Method consistency test

Prior to the analysis of the HERAS 2017 and 2018 data, a consistency test between the method employed here and the method used by (Macaulay et al. 2018) on the IBWSS 2016 data was carried out. Echogram examples of this data set are shown in Figure 8 for the EK80 CW and the EK60 at 38 kHz. Both systems show echograms of similar amplitudes. Using a subset of the IBWSS 2016 data, an EK60/EK80 CW ping to ping statistical comparison was carried out. Specifically, a linear regression of EK60/EK80 CW for each coupled Sa values (in time and depth). The results are shown in Figure 9. The resulting slope is 1.01, i.e. almost a one to one relationship between EK60 and EK80 CW results. The study by Macaulay et al. (Macaulay et al. 2018) calculated a slope of 1.0 using more samples from the same data set. One can conclude that both methods yield very similar results.

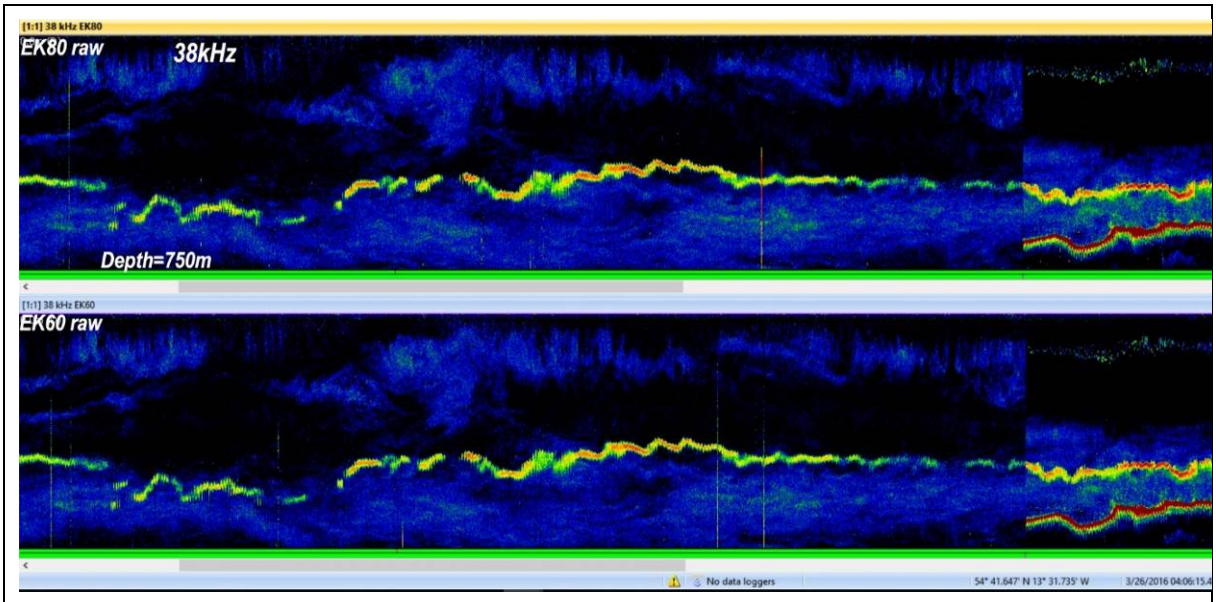

Figure 8: *A portion of the 38kHz data from 2016 IBWSS. This is the data set used for the analysis in Macaulay et al. 2018* (Macaulay et al. 2018). *Part of this region was used to reproduce the linear regression results in order to check the consistency of the two methods.*

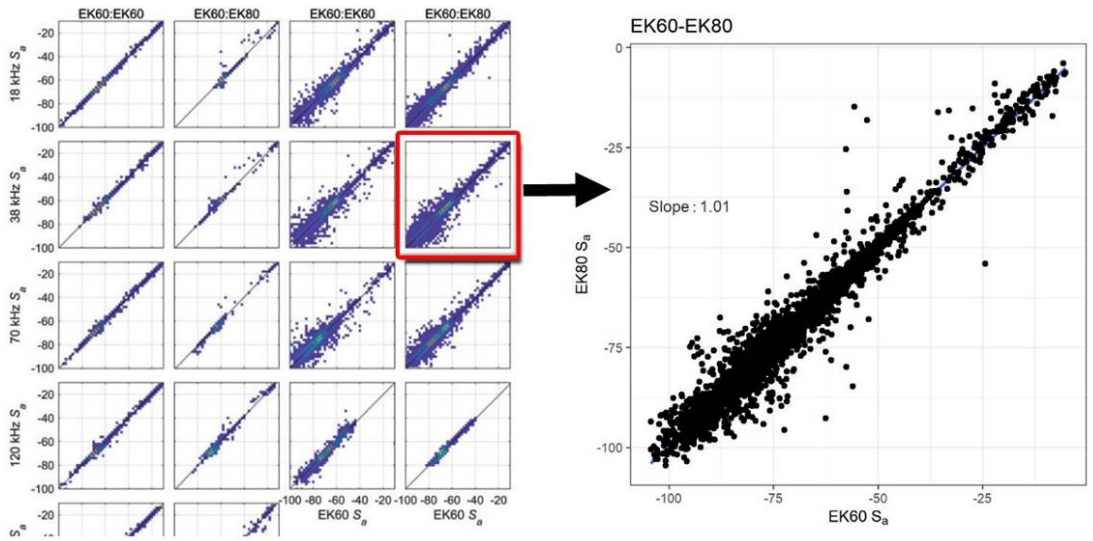

Figure 9: *Scatter plots of EK 60 versus EK80 CW Sa values. The results of this study are very similar to Macaulay et al.* (Macaulay et al. 2018)*. The left panel is a modified graph from* (Macaulay et al. 2018)*. The right panel presents the results for the 38kHz in the present study. The shape of scatter plot and the spread of data are very similar.*

3.3.2 HERAS 2017

Examples of EK60 and EK80 CW echograms from the HERAS 2017 survey are shown in Figure 10. Similar amplitude levels can be observed apart from spike noise for the EK80 CW. Results of the statistical analysis of the HERAS 2017 collected by RV Tridens II are shown in Table 1 and Figure 11 for all the frequencies. In each subplot of Figure 11, a summary of the statistics for the specific linear regression is given.

The upper part of the Table 1 shows the comparison of EK60/EK60 subsets (odd and even pings). This is representative of the stochastic variability between EK60 pings, or narrowband echosounder measurements in general. For each frequency, the slope approximates 1 with RMS errors around 1 dB. The RMS error is particularly large at 70 kHz (2.96 dB). This is due to localised intermittent spike noise. The corresponding scatter plot and fits are shown for each frequency in Figure 11. Data points corresponding to regions with spike noise can be observed for example in Figure 11(e) (data points deviating severely from regression line). It can be observed that these are not numerous, validating the manual scrutiny. An example echogram with skipe noise is shown in Figure 10. The removal of these regions would improve the level linear regression but their inclusion does not affect significantly the comparison parameters (e.g. ΔSa or the regression slope). Overall, for all channels, the P-values are large, meaning that the difference is not significant.

The lower part of the Table 1 show the comparison of the EK80 CW and EK60 pairs. The corresponding scatter plots are presented in Figure 11. As for the EK60/EK60 ping to ping comparison, the 70 kHz channel shows deviations due to regions with intermittent spike noise. However, this does not affect the P-value. Overall, for all frequency channels the EK80 CW yielded similar results to the EK60, suggesting both systems are equivalent.

Table 1: *summary results of the analysis conducted on the HERAS 2017 data. This includes the variability between EK60 pings (upper table) and the comparison between EK60 and EK80 CW (lower table).*

2017 EK60_even / EK 60_odd							
Frequency	RMS error	T-value	P-value	Δ Sa	R^2	Slope	N samples
18kHz	0.86	-0.58	0.5639	0.02	0.98	0.984	5888
38kHz	0.94	-0.67	0.5018	0.03	0.98	0.985	5888
70kHz	2.96	-0.46	0.6451	0.01	0.92	0.954	5888
120kHz	1.27	-0.5	0.6173	0.04	0.96	0.968	5888
200kHz	0.97	-0.79	0.4322	0.06	0.97	0.977	5888
2017 EK60 / EK 80							
Frequency	RMS error	T-value	P-value	Δ Sa	R^2	Slope	N samples
18kHz	2.7	-0.21	0.8333	0.42	0.93	0.918	5891
38kHz	0.66	-0.37	0.7147	0.27	0.99	1.008	5706
70kHz	5.11	-0.94	0.3476	0.04	0.87	0.937	5891
120kHz	2.41	-0.45	0.6547	0.58	0.93	0.993	5891
200kHz	0.62	0.85	0.3979	0.59	0.98	1.009	5891

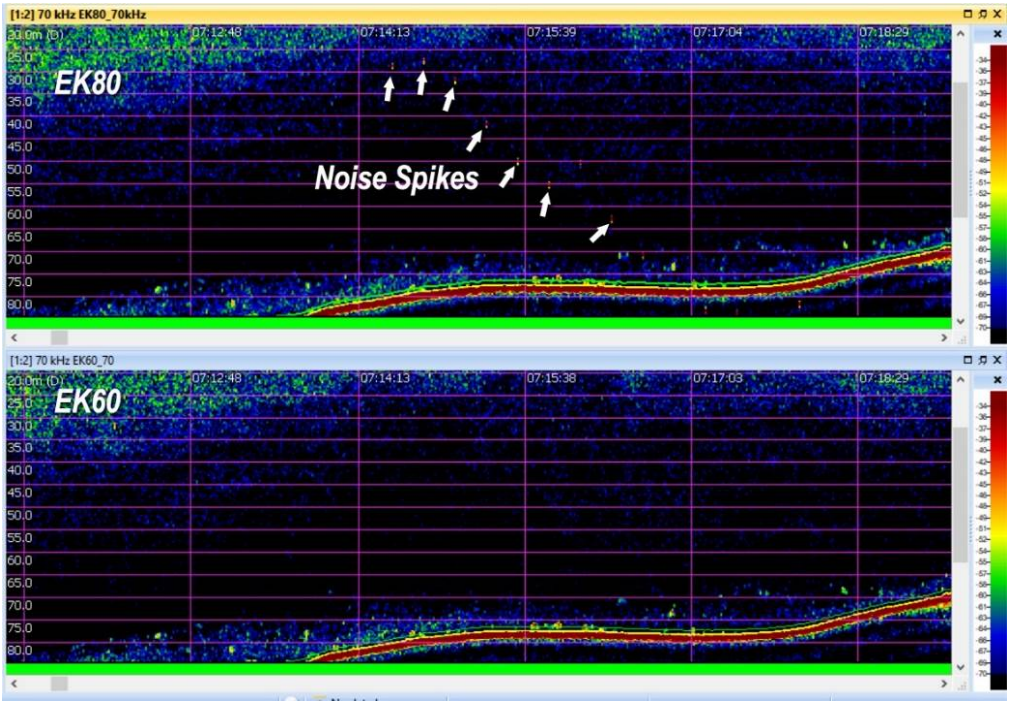

Figure 10: *Example of intermittent noise spikes in the 70 kHz that cause discrepancies between some pairs. In this example the noise is visible only on EK80 and not on EK60. There are other sections where the opposite is also the case.*

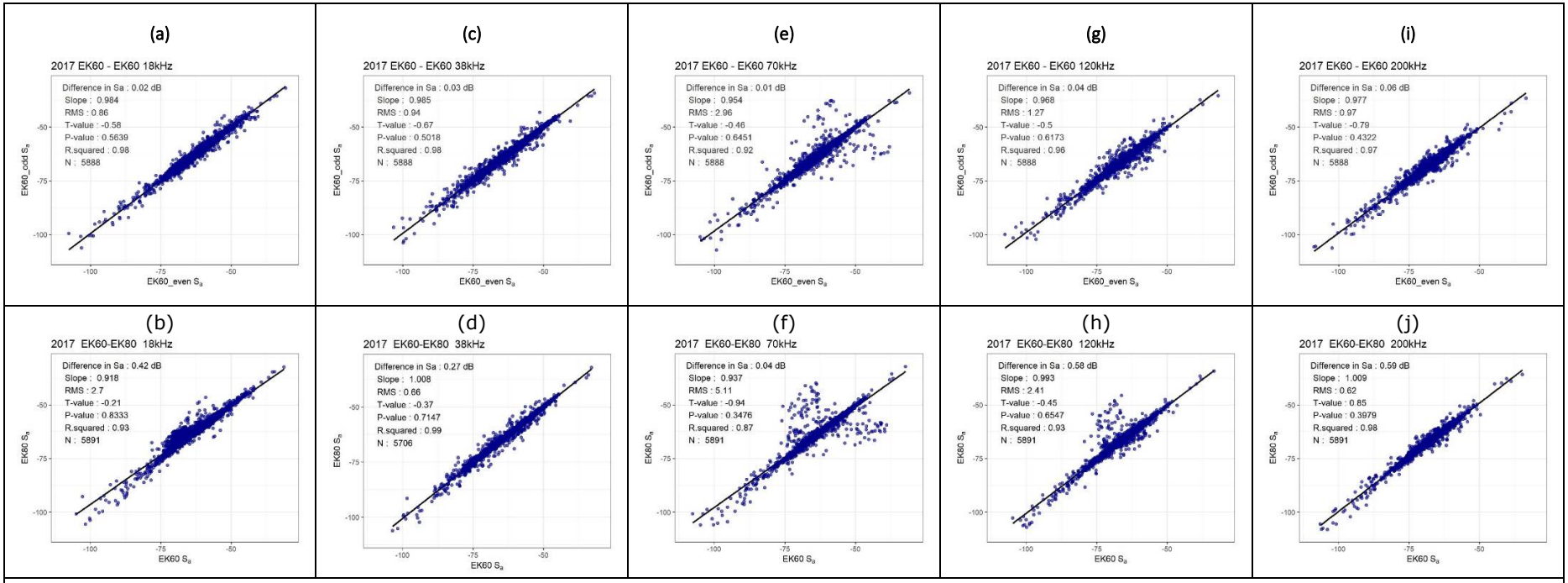

Figure 11: *Two-dimensional histogram of area backscattering strength (Sa) cell pairs from the EK60_even to EK60_odd and EK60 to EK80 CW for the analysis of the HERAS 2017 data. (a) and (b) 18 kHz. (c) and (d) 38 kHz. (e) and (f) 70 kHz. (g) and (h) 120 kHz. (i) and (j) 200 kHz. The 70 kHz channel (e and f) and 120 kHz for the EK80 CW (h) show deviations due to regions with intermittent spike noise, without affecting the P-value.*

3.3.3 HERAS 2018

Results of the analysis of the HERAS 2018 collected by RV Tridens II are shown in Table 2 and Figure 12 for all the frequencies. In each subplot of Figure 12, a summary of the statistics for the specific linear regression is given.

The comparison of EK60/EK60 subsets (i.e. the odd and even pings) is shown in Table 2. Compared to the analysis of the HERAS 2017 data (Table 1), the RMS error is overall higher for all frequencies. This can be explained by the difference in data collected between 2017 and 2018. During HERAS 2017, ping to ping data were collected during inter-transects while during HERAS 2018, ping to ping data were collected during survey transects and around fishing operations. One expects natural variability in Sa and this is most likely dependent on Sa levels (i.e. the higher the Sa values the higher the variability). In addition, the data recorded during HERAS 2018 were further North where herring is usually observed in dense marks. In short, the HERAS 2018 data set exemplify strong acoustic marks as opposed to the HERAS 2017 data set. Furthermore, the number of data points in 2018 is twice the size of the 2017. However, for all channels, the P-values are large, meaning that the difference between Sa cell pairs is not significant.

The comparison between EK60 and EK80 CW (lower part of Table 2) shows potential discrepancies at 18 kHz and 38 kHz. For 70 kHz, 120 kHz and 200 kHz, the EK60 and the EK80 CW yield similar results, in line with the previously observed stochasticity. The discrepancy between EK60 and EK80 CW is particularly strong at 38 kHz and is in line with what was observed with the results from the calibration trials (Section 2, Figure 5). This can be observed in Figure 12(d).

Table 2: *Summary results of the analysis conducted on the HERAS 2018 data. This includes the variability between EK60 pings (upper part) and the comparison between EK60 and EK80 CW (lower part).*

2018 EK60_even / EK 60_odd							
Frequency	RMS error	T-value	P-value	Δ Sa	R^2	Slope	N samples
18kHz	1.71	0.1	0.9171	0.01	0.95	0.976	11291
38kHz	3.72	-0.11	0.9155	0.01	0.92	0.963	11190
70kHz	2.65	-0.14	0.8897	0.05	0.93	0.957	11290
120kHz	2.72	0.31	0.7544	0.03	0.9	0.953	11290
200kHz	2.86	0.08	0.9368	0.03	0.89	0.946	11290
2018 EK60 / EK 80							
Frequency	RMS error	T-value	P-value	Δ Sa	R^2	Slope	N samples
18kHz	8.07	3.11	0.0019	2.59	0.76	0.837	11351
38kHz	10.06	4.18	<0.0001	5.54	0.57	0.534	11237
70kHz	2.79	-0.3	0.766	0.49	0.92	0.971	11350
120kHz	2.83	-0.03	0.98	1.13	0.91	1.021	11355
200kHz	2.84	0.97	0.3321	0.31	0.9	0.975	11353

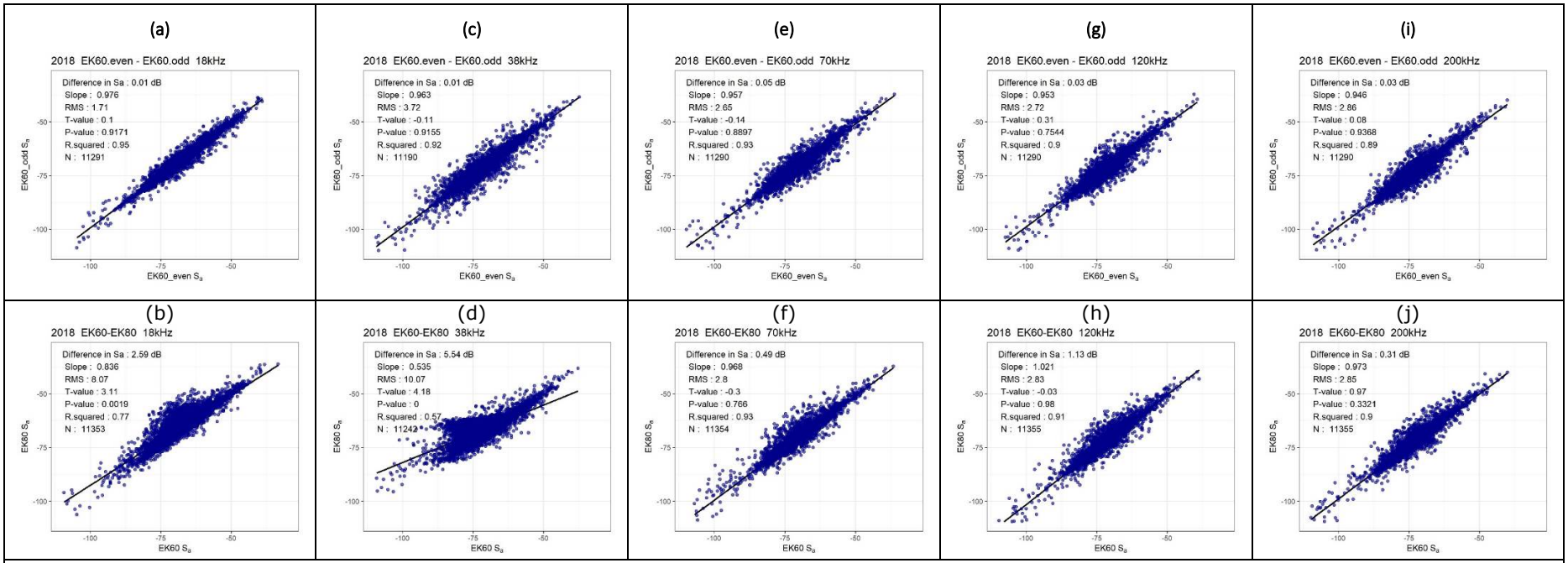

Figure 12: *Two-dimensional histogram of area backscattering strength (Sa) cell pairs from the EK60_even to EK60_odd and EK60 to EK80 CW for the analysis of the HERAS 2018 data. (a) and (b) 18 kHz. (c) and (d) 38 kHz. (e) and (f) 70 kHz. (g) and (h) 120 kHz. (i) and (j) 200 kHz.*

3.3.4 *Discussion*

For both the HERAS 2017 and 2018 data sets, the EK60_even to EK60_odd comparison shows results in line with the stochasticity expected from an echosounder. The slope of each regression (upper parts in Table 1 and Table 2) is around 1. The somewhat higher level of RMS error observed for the HERAS 2018 data is due to the presence of stronger acoustic marks in the data set compared to the HERAS 2017 data.

As for the comparison between the EK60 and the EK80 CW, the analysis of the HERAS 2017 data yields similar results to (Macaulay et al. 2018). However, the HERAS 2018 data show discrepancies for both the 18 kHz and 38 kHz channel. The discrepancy is particularly large at 38 kHz where EK60 and EK80 CW results deviate significantly (Figure 12(d)). The timing of HERAS 2018 (June/July 2018) is in line with the abrupt change in calibration gain observed in Section 2.

The discrepancy at 38kHz between the EK60 and the EK80 CW is of particular relevance because this channel is most often used for abundance estimation during surveys. Other channels than 38 kHz are used by the survey analyst for identification of features in the water column (e.g. differentiation between fish species, identification of plankton layers). Therefore, the consistency of the 38 kHz is far more critical than the other frequencies. In Macaulay et al. (Macaulay et al. 2018) (Table 3), the EK60/EK80 CW pair at 38kHz for RV Tridens II exemplifies an RMS error of 0.9 dB and a regression slope of 1.00. For the HERAS 2017 data, the RMS error is 0.7 dB and the slope is 1.01 (Table 1). A significant change occurred in the HERAS 2018 data with an RMS error of 10.06 dB and a slope of 0.534 (Table 2). While differences in RMS errors of 1-2 dBs can a result of the distribution of the backscatter (e.g. lack of spatial homogeneity in the targets, stronger targets in the data), the increase in RMS error from 0.7 dB to 10.06 dB from 2017 to 2018 is suspicious. The calibration results presented in Section 2 (Figure 5) support a potential problem with the 38 kHz EK80 CW transceivers on board RV Tridens II. An investigation of the HERAS 2017 data was performed and revealed a discrepancy in transducer impedance for quadrant 2 starting on 13th July around 03:35 AM (Figure 13). Beyond this point, a higher noise floor could be observed in the 38 kHz echogram of the EK80 CW, especially beyond the 40 m mark. The depth dependency of this discrepancy will be further investigated below.

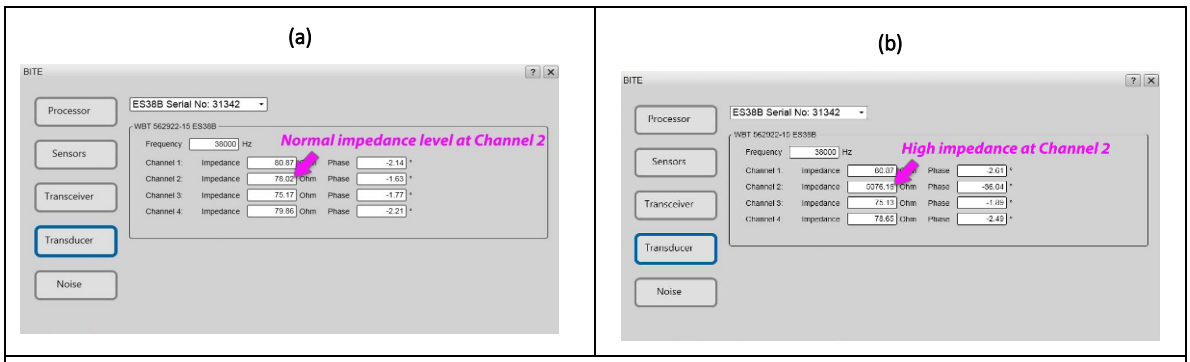

Figure 13: *Screenshot of transducer impedance observed in two different HERAS 2017 data files. (a) impedance on 13th July 03:34 AM. (b) erroneous impedance appear on 13th July 03:35 AM onward.*

Though the extent of the discrepancy observed at 18 kHz is less than the one observed at 38 kHz, it remains an unusual deviation that requires further investigation. First, it is important to note that this deviation is only observed for the HERAS 2018 data (Table 2 and Figure 12). The analysis of the HERAS 2017 (Table 1 and Figure 12) gives comparable results between the EK60 and the EK80 CW. Close scrutiny of the HERAS 2018 reveals two potential sources for the observed discrepancy. Echogram examples of these are shown in Figure 14. First, the area of acoustic ring down (post-peak reverberation) near the transducer is different for the EK60 and the EK80 CW (Figure 14(a), see the near surface region). The

source of this difference could either be: 1) Varying EK80 CW settings or electrical problems (e.g. due to the multiplexer). This needs to be further investigated. 2) Noise interferences from other acoustic equipment (e.g. omnidirectional sonar used on board was observed). This is shown in Figure 14(b) with the appearance of noise stripes for the EK80 CW. This was only observed for recordings during fishing operations, i.e. when other acoustic equipment than EK60 and EK80 CW were switched on. The sensitivity of the EK80 CW to external noise sources is potentially due to the use of a higher bandwidth.

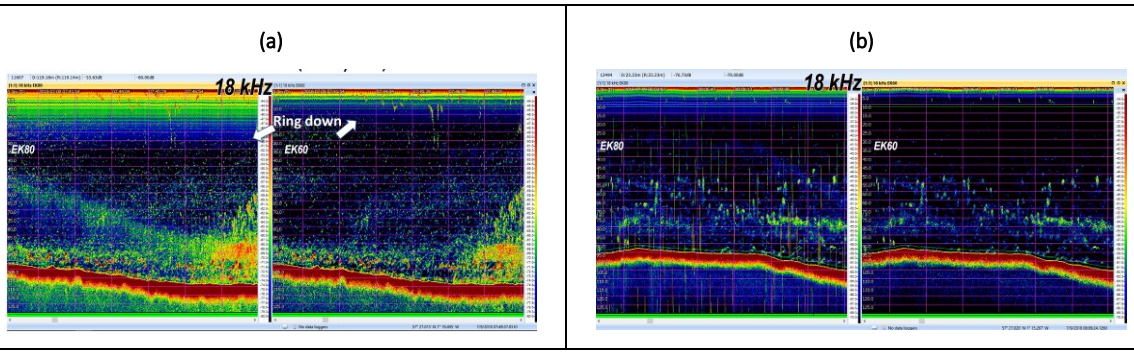

Figure 14: *echograms exemplifying the discrepancies observed between the EK60 and the EK80 CW systems at 18 kHz. (a) Discrepancy between EK60 and EK80 CW due to different extend of the ring down area below the transducer. This is observable a few meters below the water surface with a higher noise floor for the EK80 CW. (b) Discrepancy between EK60 and EK80 CW due to acoustic noise interferences. The interferences consist of stripes that are only visible on the EK80 CW, probably due to a larger bandwidth for this system.*

Despite the similarities observed in the scatterplots (Figure 11 and Figure 12), there seems to be variations with depth in the EK60/EK80 CW data set. This was also observed by Macaulay et al. (Macaulay et al. 2018) who hypothesize that such variability could originate from the differences in the way that sound speed and absorption coefficients are calculated in these two different systems. Also, it is known that the EK80 CW is more a sensitive device (showing more extensive background noise). It is worthwhile to look at the effect of depth for the data available here. The results are presented in Figure 15 and Figure 16. In these plots, the median, 25th percentile and 75th percentile of the Δ Sa in time are plotted for every 5 m depth separations. Results are shown for the EK60_even to EK60_odd and EK60 to EK80 CW comparisons. Using the EK60_even to EK60_odd plots as a baseline for each frequency channel, one can observe the similarities between EK60 and EK80 CW at different depths. It is important to mention that, at depths greater than ~120 m, only few data points are available because the depth range covered by the HERAS survey is mostly below this depth. Thus the results greater than ~120 m are not representative of a large sample and should be disregarded. Overall, the depth dependence is varying for the different frequency channels:

- 18 kHz: for the analysis of both the HERAS 2017 and 2018 data, a deviation in the shallow region (Figure 15 (b) and Figure 16 (b), below ~40 m) can be observed. This variability is driven by the larger ring down region of the EK80 CW (Figure 14(a)). The deviations at larger depth (below 120 m) for the HERAS 2018 data (Figure 16 (b)) are due to noise interferences of other acoustic equipment used during fishing operations.
- 38 kHz: there is a good agreement for the HERAS 2017 dataset (Figure 15 (d)). However, a large offset is observed for the HERAS 2018 data (Figure 16 (d)), as observed in the linear regression (Table 2 and Figure 12). This is due to the malfunctioning of the EK80 transceiver and no conclusion can be drawn from Figure 16 (d).
- 70 kHz: there is a slight but negligible offset effect of depth in for the HERAS 2017 (Figure 15 (f)). Results from the analysis of the HERAS 2018 data (Figure 16 (f)) start with a similar offset at shallow depths.
- 120 kHz: the results from the analysis of the HERAS 2017 data (Figure 15 (h)) show a offset in favour of EK60 of 0.5 dB at the surface and reaches almost 1 dB at 100m. A similar trend is observed for HERAS 2018 data (Figure 16(h)) with a starting offset of 1 dB reaching 1.5 dB at 100 m.

- 200kHz: Results from the HERAS 2017 data shows an offset in favour of the EK80 CW of 0.5-1 dB (Figure 15(j)). This remains consistent until 120 m. However for HERAS 2018 data (Figure 16(j)), there is a 0.5 dB offset near surface in favour of EK60 followed by an increasing trend, ending with an offset of 1.5 dB in favour of the EK80 CW around 120 m depth.

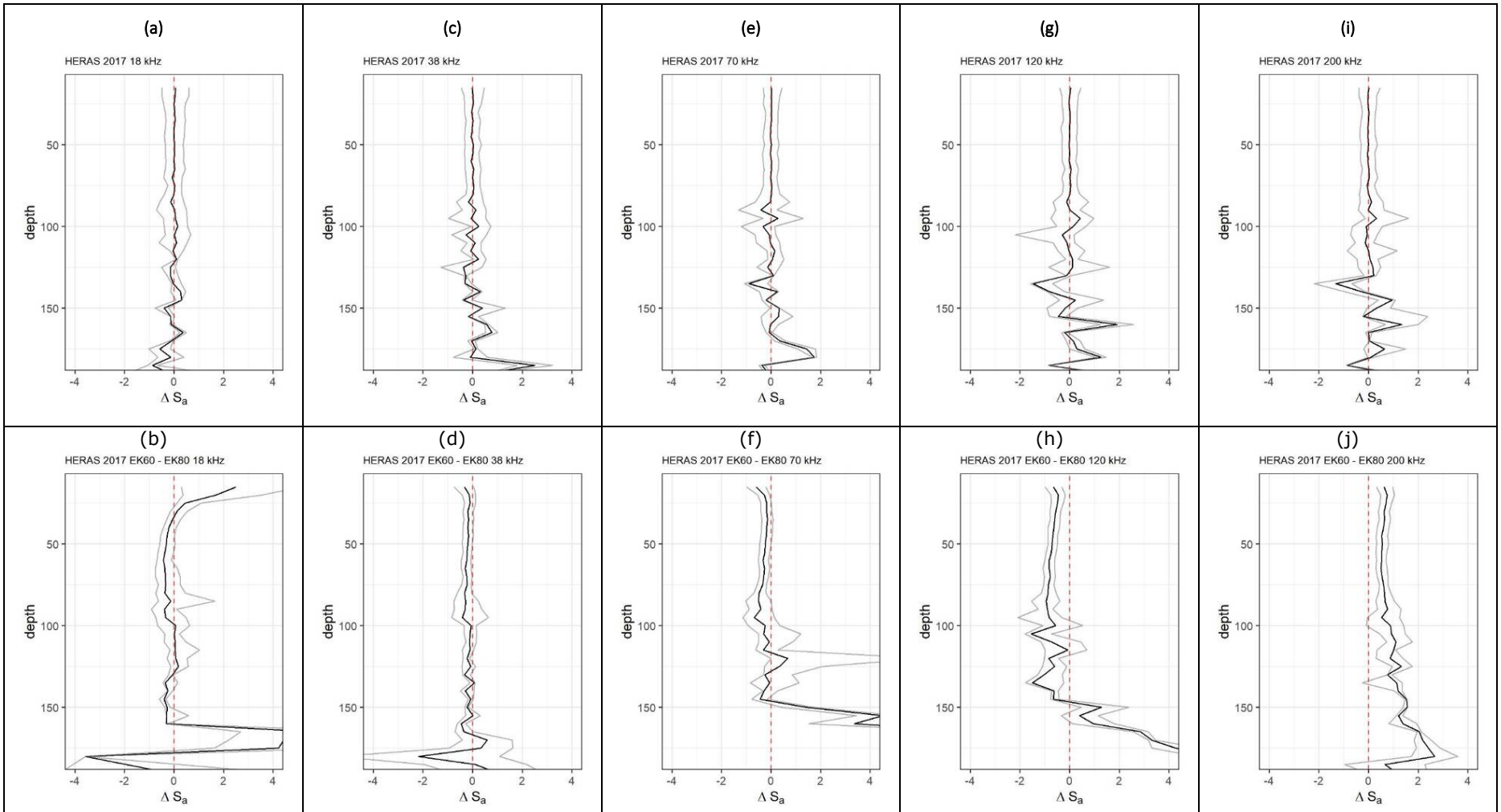

Figure 15: *Depth dependence in 2017. The figure shows the median, 25th percentile and 75th percentile of the Δ Sa plotted as lines connecting the values at every 5 m. depth bins. The top panels show the EK60_EVEN to EK60_ODD plots and bottom panels show the EK60/EK80.*

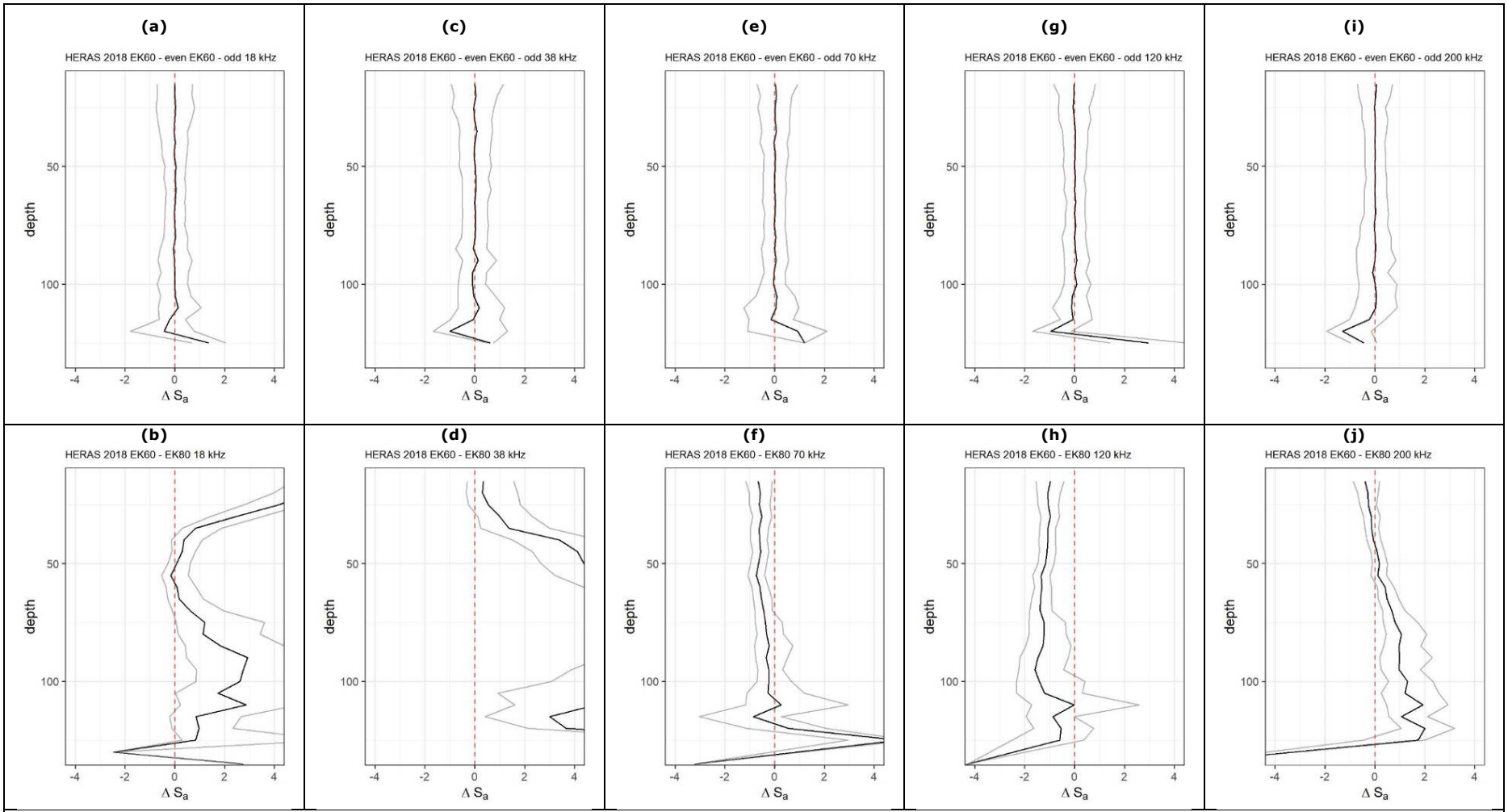

Figure 16: *Depth dependence in 2018. The figure show the median, 25th percentile and 75th percentile of the Δ Sa plotted as lines connecting the values at every 5 m. depth bins. The upper panels show the EK60_EVEN to EK60_ODD plots and bottom panels show the EK60/EK80.*

4 Conclusions

In this study, the use of the EK80 CW echosounder for routine acoustic surveys was investigated. This is motivated by the fact that the echosounder currently used for acoustic surveys (EK60) is no longer manufactured by Simrad and is superseded by the EK80 CW. Several studies suggest that both systems are equivalent (Macaulay et al. 2018; Demer et al. 2017; ICES 2017, 2018a; Sakinan et al. 2018). However, it is important to perform platform specific investigations when possible. This study present results specific to RV Tridens II. On this vessel, WMR currently uses the EK60 for routine surveys and results presented here aim at initiating the change from EK60 to the EK80 CW

First, calibration records for the EK80 CW are investigated. This consists of the gathering of historical results since 2015 and the automatic generation of tables and plots for each calibration trial together with resulting gain. This investigation revealed a discrepancy for the EK80 CW 38 kHz channel appearing between June 2017 and March 2018. This highlights the need for an efficient way to revisit survey historical results. To that aim, the data management and R codes developed here will be used to produce an updated calibration report after each survey in the future. This will allow one to track suspicious changes in the sensitivity of the EK80 CW.

Second, on board RV Tridens II, a multiplexer, allowing one to collect ping to ping data between EK60 and EK80 CW, was installed to that purpose. Subsequently, large amount of ping to ping data were collected during IBWSS 2016, HERAS 2017 and 2018. The data from IBWSS 2016 were analysed and presented in (Macaulay et al. 2018) and the present study further the investigation to the HERAS 2017 and HERAS 2018 data. Results derived from the HERAS 2017 data show that the EK60 and EK80 CW produce similar results for all frequency channels. However, the analysis of the HERAS 2018 revealed very large discrepancies for the 38 kHz channel. The origin of the issue was tracked down to 13th July 2017 and is due to the malfunctioning of the EK80 transceiver. Though of lesser importance and amplitude, the results of the 18 kHz channels also exemplified small deviations between EK60 and EK80 CW. Though minor, the issue with the 18 kHz channel originates from noise interference and near surface reflections that are stronger with the EK80 CW. This could be due to a difference in setting with the EK80 CW and it will need to be further investigated during the next surveys. However, the discrepancy for the 38 kHz channel is problematic in its scale but also because of the importance of this frequency channel for acoustic surveys. The erroneous acoustic measurements are coming from a malfunctioning of a quadrant for the EK80 CW. This problem must be solved prior to changing from EK60 to EK80 CW for survey purposes.

Overall, results from various studies and recommendations from working groups (ICES 2017, 2018a; Macaulay et al. 2018; Sakinan et al. 2018; Demer et al. 2017) showed that the EK60 and the EK80 CW produce comparable results. The differences found can be mostly repaired with the investigations in this report. However, this study also revealed a malfunctioning with the 38 kHz channel but also confirmed that in the case of RV Tridens II, once the malfunctioning is solved, it is safe to change from EK60 to EK80 CW for the collection of data during acoustic surveys.

References

Dalen, John, and Odd Nakken. 1983. "On the Application of the Echo Integration Method." ICES CM 1983/B: 19.

Demer, D. A., L. N. Andersen, C. Bassett, L. Berger, D. Chu, J. Condiotty, G. R. Cutter, et al. 2017. "2016 USA–Norway EK80 Workshop Report: Evaluation of a Wideband Echosounder for Fisheries and Marine Ecosystem Science." In *ICES Cooperative Research Report*, 336:69. http://doi.org/10.17895/ices.pub.2318.

Demer, D. A., L. Berger, M. Bernasconi, E. Bethke, K. Boswell, D. Chu, R. Domokos, et al. 2015. "Calibration of Acoustic Instruments." *ICES Cooperative Research Report* 326: 133.

Foote, K. G., H. P. Knudsen, G. Vestnes, D. N. MacLennan, and E. J. Simmonds. 1987. *Calibration of Acoustic Instruments for Fish Density Estimation : A Practical Guide*. Copenhagen Denmark: International Council for the Exploration of the Sea.

Foote, Kenneth G. 1982. "Optimizing Copper Spheres for Precision Calibration of Hydroacoustic Equipment." *The Journal of the Acoustical Society of America* 71 (3): 742. https://doi.org/10.1121/1.387497.

Hobæk, Halvor, and Tonje Lexau Nesse. 2006. "Scattering from Spheres and Cylinders - Revisited." In *29th Symposium on Physical Acoustics*. Norwegian Physical Society. http://hdl.handle.net/1956/3879.

ICES. 2015. "Manual for International Pelagic Surveys (IPS)."

ICES. 2017. "Interim Report of the Working Group on Fisheries, Acoustics, Science and Technology." In *WGFAST 2017*, 40. 4-7 April 2017. Nelson, New Zealand, ICES CM 2017/SSGIEOM:12.

ICES. 2018a. "Interim Report of the Working Group on Fisheries Acoustics, Science and Technology (WGFAST)."

ICES. 2018b. "Report of the Working Group on International Pelagic Surveys (WGIPS)."

Jech, J. M., K. G. Foote, D. Chu, and L. C. Hufnagle Jr. 2005. "Comparing Two 38-KHz Scientific Echosounders." *ICES Journal of Marine Science* 62 (6): 1168–79. https://doi.org/10.1016/j.icesjms.2005.02.014.

Korneliussen, Rolf J., Yngve Heggelund, Gavin J. Macaulay, Daniel Patel, Espen Johnsen, and Inge K. Eliassen. 2016. "Acoustic Identification of Marine Species Using a Feature Library." *Methods in Oceanography* 17 (December): 187–205. https://doi.org/10.1016/J.MIO.2016.09.002.

Macaulay, Gavin J, Ben Scoulding, Egil Ona, and Sascha M M Fässler. 2018. "Comparisons of Echo-Integration Performance from Two Multiplexed Echosounders." *ICES Journal of Marine Science* 75 (6): 2276–85. https://doi.org/10.1093/icesjms/fsy111.

Maclennan, D, Paul G. Fernandes, and John Dalen. 2002. "A Consistent Approach to Definitions and Symbols in Fisheries Acoustics." *ICES Journal of Marine Science* 59 (2): 365–69. https://doi.org/10.1006/jmsc.2001.1158.

MacLennan, David. 1981. "The Theory of Solid Spheres as Sonar Calibration Targets." *Scottish Fisheries Research Report*, no. 22.

Mehl, Sigbjørn, Espen Johnsen, Åsmund Skålevik, and Asgeir Aglen. 2018. "Estimation of Acoustic Indices with CVs for Northeast Arctic Saithe in the Norwegian Coastal Survey 2003-2017 Applying the Sea2Data StoX Software." *19*. Fisken og Havet;1-2018: Institute of Marine research, Bergen, Norway. https://brage.bibsys.no/xmlui/handle/11250/2562514.

NOAA. 2004. "EK500-EK60 Comparison Workshop."

Sakinan, Serdar, Dick de Haan, Dirk Burggraaf, and Sacha Fassler. 2018. "Investigation of Echosounder Finger Prints of Dutch Pelagic Freezer Trawlers (SEAT II) Evaluation of the SEAT II Joint-Industry Project : Evaluation of the SEAT II Joint-Industry Project." https://library.wur.nl/WebQuery/wurpubs/541398.

Simmonds, E John, and D N MacLennan. 2005. *Fisheries Acoustics : Theory and Practice*. *Fish and Aquatic Resources Series ;* 2nd ed. Oxford ; Ames, Iowa: Blackwell Science.

Quality assurance

CVO is certified to ISO 9001:2015 (certificate number: 268632-2018-AQ-NLD-RvA). This certificate is valid until December 15th, 2021. The certification was issued by DNV GL Business Assurance B.V

Justification

CVO Report: 20.014
Project number: 4311300061

The quality of this report has been peer reviewed by a colleague scientist and the head of CVO.

Approved by:	Mr. A.S. Couperus DLO HBO Researcher
Signature:	
Date:	19/06/2020
Approved by:	Ms. Dr. C.J.G. van Damme DLO Researcher
Signature:	
Date:	19/06/2020
Approved by:	Mr. Ing. S.W. Verver Head Centre for Fisheries Research
Signature:	
Date:	19/06/2020

Annex I: EK80 calibration results

The results of each calibration test are presented as summary tables below. The tables contain information such as, gain, Sa correction and beam pattern parameters. Additional meta-data are also included such as software, firmware, date, time, number of hits and the type of the calibration sphere.

The tables are followed by subsequent scatter plots of the calibration hits, representative of position of the sphere relative to the centre of the acoustic beam and the error of each measurement point. The error (square of the difference of the measurement relative to the expected Target Strength of the sphere) is visualized on a colour scale.

On these scatter plots, the concentric circles show the angular positions relative to the centre of the beam as 1°, 3.5° and 5 °. In addition, the necessary calibration parameters are given as text annotations.

In the last section are time series plots showing the results for EK60 and EK80 CW for each calibration experiment for each frequency. The box plots show the spread of the measurements. The line plots with RMS error whiskers show the TS gain determined as final outputs. The comparison of EK80 CW and EK60 gives a baseline for comparison. For example, if a sharp change is observed equally in both systems, then it means that the reason is most likely transducer originated. However if this is only observed in one of the systems, then the reason is probably the transceiver (as in the case of 38 kHz echosounder here).

I.1 Calibration June 2018 Scapa Flow

Table I.1: *Calibration Results*

parameter	ES18	ES38B	ES70-7C	ES120-7C	ES200-7C
Frequency	18000	38000	70000	120000	200000
Gain	23.19	25.63	27.96	27.53	27.22
SaCorrection	0.0003	-0.0321	-0.0557	-0.1208	-0.2621
BeamWidthAlongship	10.26	7.14	6.47	6.09	6.55
BeamWidthAthwartship	10.52	7.11	6.42	6.04	6.51
TsRms	0.0843	0.1929	0.3376	0.2951	0.0574
Pulse Length	1.024	1.024	1.024	1.024	1.024
Software	1.12.2.0	1.12.2.0	1.12.2.0	1.12.2.0	1.12.2.0
Firmware	2.20	2.20	2.20	2.20	2.20
Date	2018-June-27	2018-June-27	2018-June-28	2018-June-27	2018-June-27
Time	13:09:35	15:06:40	16:24:03	15:52:51	20:46:03
No of hits	2991	1519	1728	1294	935
Sphere	Copper (Cu) 63mm	Tungsten (WC-Co) 38.1mm	Tungsten (WC-Co) 38.1mm	Tungsten (WC-Co) 38.1mm	Tungsten (WC-Co) 38.1mm

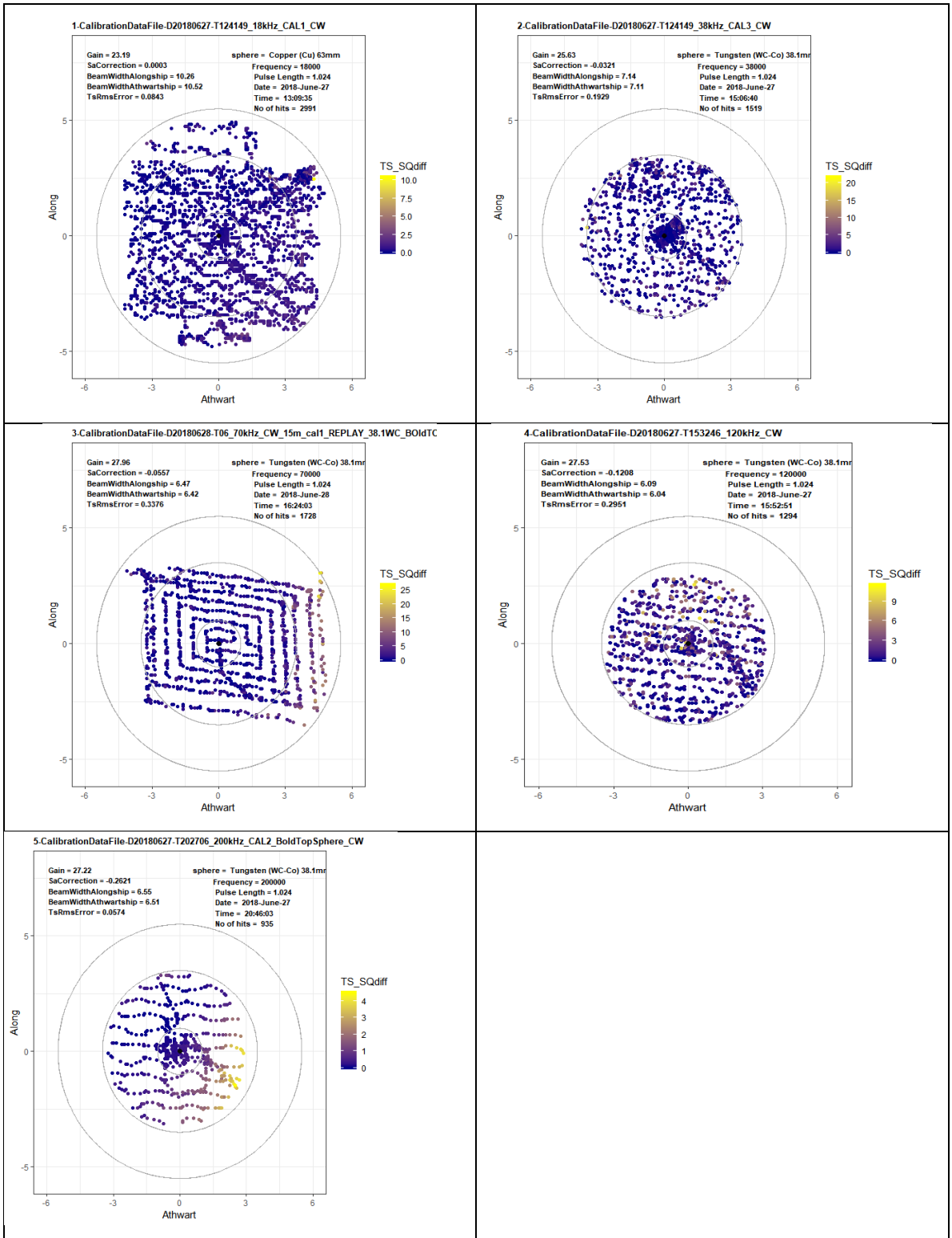

Figure I.1: *Calibration June 2018 Scapa Flow (HERAS) beam coverage and TS deviation for each target hit at different frequencies.*

I.2 Calibrations March 2018 Bantry Bay

Table I.2: *Calibration Results*

parameter	ES38B	ES70-7C	ES120-7C	ES200-7C	ES200-7C_V2
Frequency	38000	70000	120000	200000	200000
Gain	25.54	27.90	27.09	26.95	27.03
SaCorrection	-1.7776	-0.1305	0.0152	0.0821	-0.1547
BeamWidthAlongship	7.16	7.01	6.13	6.62	6.26
BeamWidthAthwartship	7.18	6.97	6.12	6.24	6.44
TsRms	0.0439	0.0455	0.0425	0.0954	0.1367
Pulse Length	1.024	1.024	1.024	1.024	1.024
Software	1.12.1.0	1.12.1.0	1.12.1.0	1.12.1.0	1.12.1.0
Firmware	2.20	2.20	2.20	2.20	2.20
Date	2018-March-15	2018-March-15	2018-March-15	2018-March-15	2018-March-15
Time	10:38:32	12:20:58	13:04:38	13:38:50	14:19:03
No of hits	780	688	1069	748	806
Sphere	Tungsten (WC-Co) 38.1mm	Tungsten (WC-Co) 38.1mm	Tungsten (WC-Co) 38.1mm	Tungsten (WC-Co) 38.1mm	Tungsten (WC-Co) 38.1mm

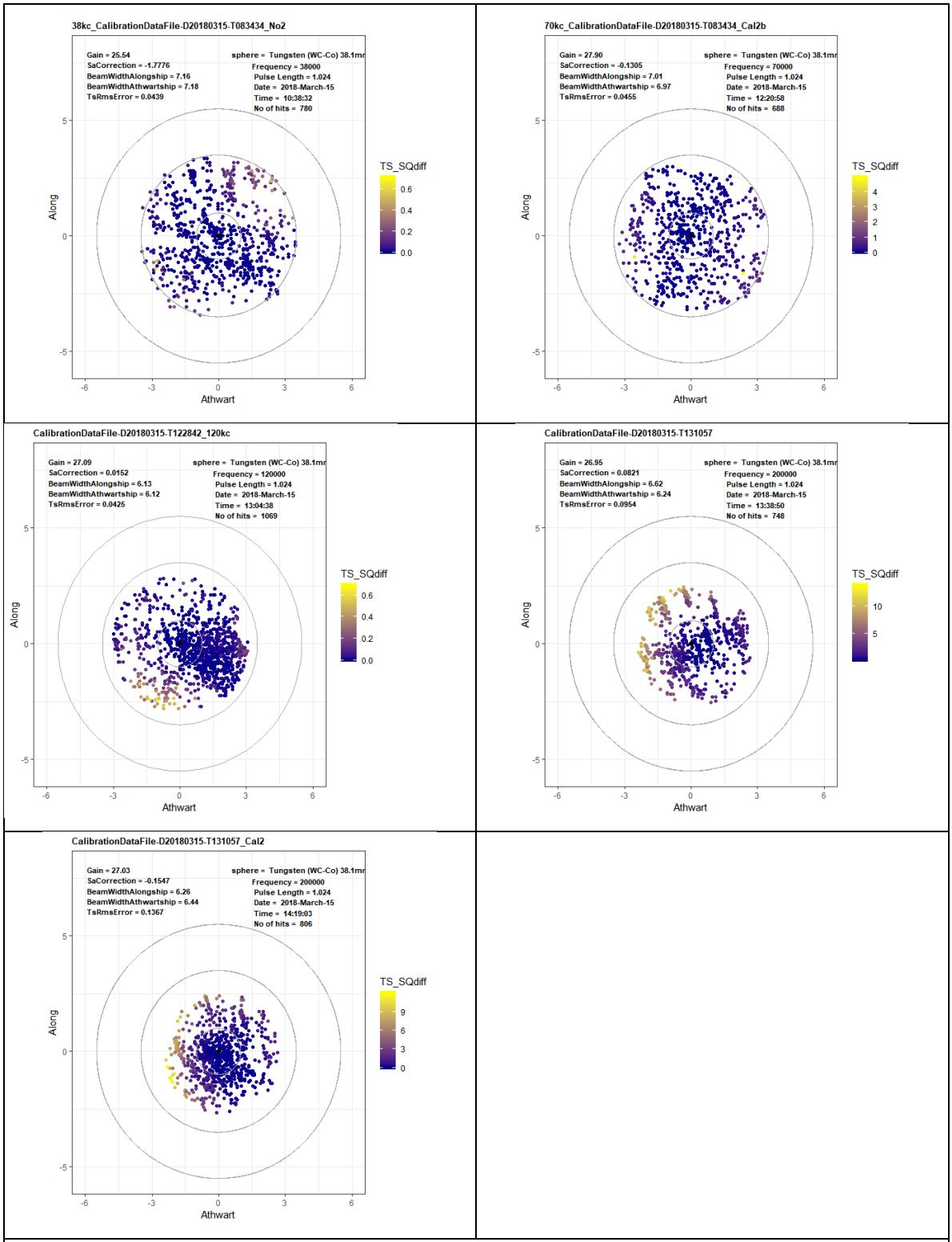

Figure I.2: *Calibration March 2018 Bantry Bay (IBWSS) beam coverage and TS deviation for each target hit at different frequencies.*

I.3 Calibration June 27 2017 ScapaFlow

Table I.3: *Calibration Results*

parameter	ES18	ES38B	ES70-7C	ES120-7C	ES200-7C	ES333-7C
Frequency	18000	38000	70000	120000	200000	333000
Gain	23.30	27.25	27.80	27.09	26.75	25.86
SaCorrection	0.0121	-1.7771	-0.1071	-0.0753	-0.1476	-0.0471
BeamWidthAlongship	10.13	6.72	6.71	6.40	6.94	4.98
BeamWidthAthwartship	10.43	6.64	6.58	6.56	6.60	5.09
TsRms	0.1450	0.1937	0.1193	0.0995	0.1492	0.3724
Pulse Length	1.024	1.024	1.024	1.024	1.024	1.024
Software	1.10.3.0	1.10.3.0	1.10.3.0	1.10.3.0	1.10.3.0	1.10.3.0
Firmware	2.16	2.16	2.16	2.16	2.16	2.16
Date	2017-June-28	2017-June-28	2017-June-28	2017-June-28	2017-June-28	2017-June-29
Time	20:29:41	21:17:02	22:08:45	22:40:25	23:16:44	20:25:53
No of hits	3976	1929	2190	3425	2430	2824
Sphere	Copper (Cu) 63mm	Tungsten (WC-Co) 38.1mm	Tungsten (WC-Co) 38.1mm	Tungsten (WC-Co) 38.1mm	Tungsten (WC-Co) 38.1mm	Tungsten (WC-Co) 22mm

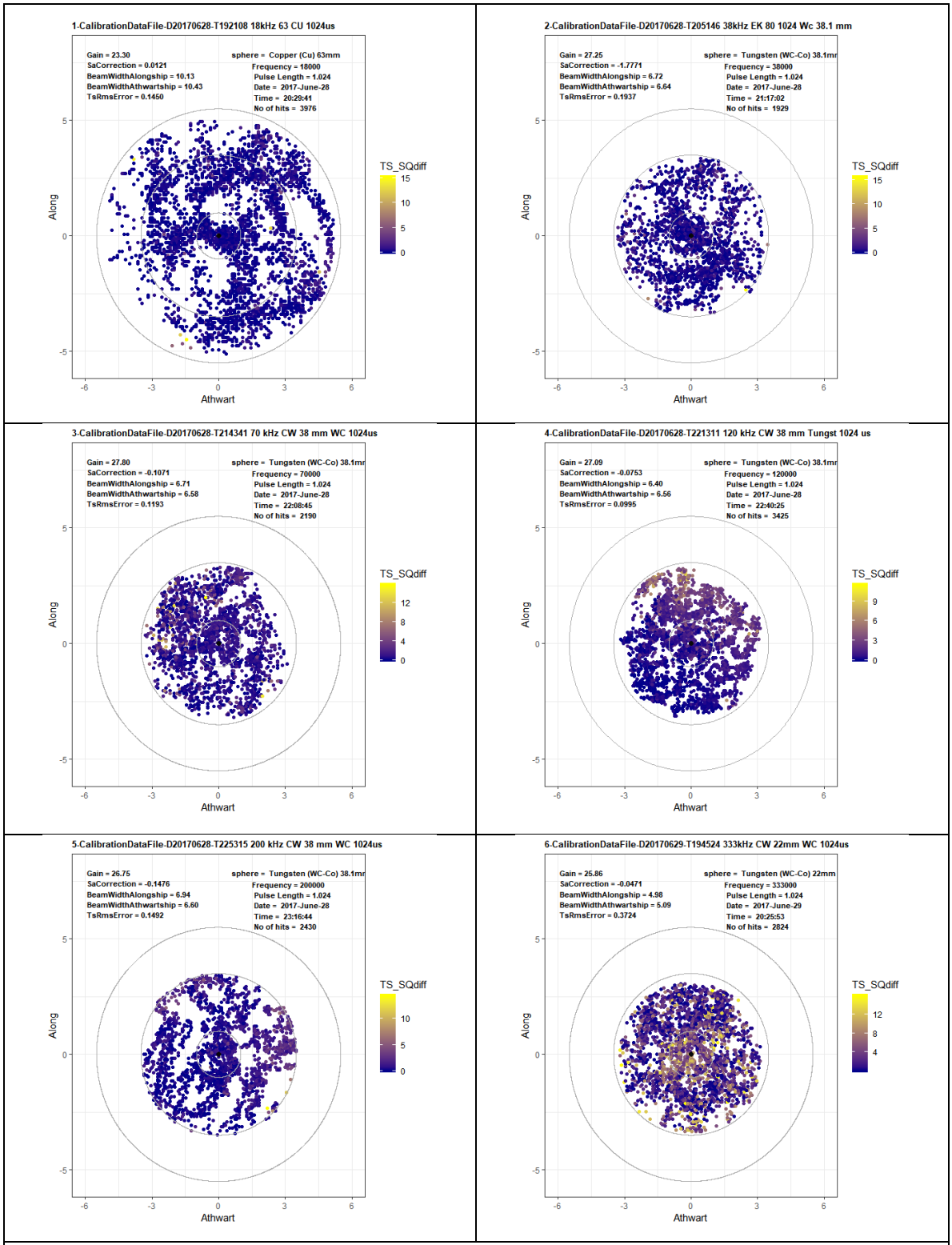

Figure I.3: *Calibration June 27 2017 ScapaFlow (HERAS) beam coverage and TS deviation for each target hit at different frequencies.*

I.4 Calibrations March 2017 Lands End

Table I.4: *Calibration Results*

parameter	ES18	ES38B
Frequency	18000	38000
Gain	23.41	27.22
SaCorrection	-0.0122	1.6433
BeamWidthAlongship	10.22	6.89
BeamWidthAthwartship	10.50	6.90
TsRms	0.0981	0.0403
Pulse Length	1.024	1.024
Software	1.10.3.0	1.10.3.0
Firmware	2.16	2.16
Date	2017-March-15	2017-March-15
Time	13:24:35	16:41:08
No of hits	830	427
Sphere	Copper (Cu) 63mm	Tungsten (WC-Co) 38.1mm

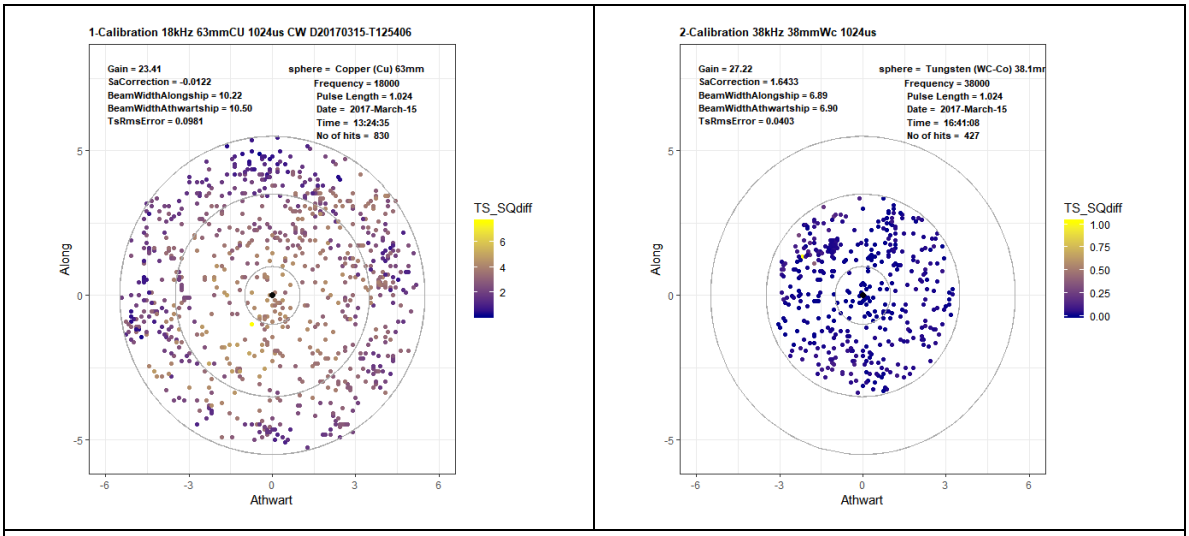

Figure I.4: *Calibration March 2017 Lands End (IBWSS) beam coverage and TS deviation for each target hit at different frequencies.*

I.5 Calibration June 2016 Scapa Flow

Table I.5: *Calibration Results*

parameter	ES18-11	ES38B
Frequency	18000	38000
Gain	23.78	27.38
SaCorrection	1.28	1.64
BeamWidthAlongship	11.62	7.22
BeamWidthAthwartship	11.65	7.22
TsRms	0.0832	0.0957
Pulse Length	1.024	1.024
Software	1.8.3.0	1.8.3.0
Firmware	1.70	1.70
Date	2016-June-29	2016-June-29
Time	11:53:24	11:34:43
No of hits	1278	860
Sphere	Copper (Cu) 63mm	Tungsten (WC-Co) 38.1mm

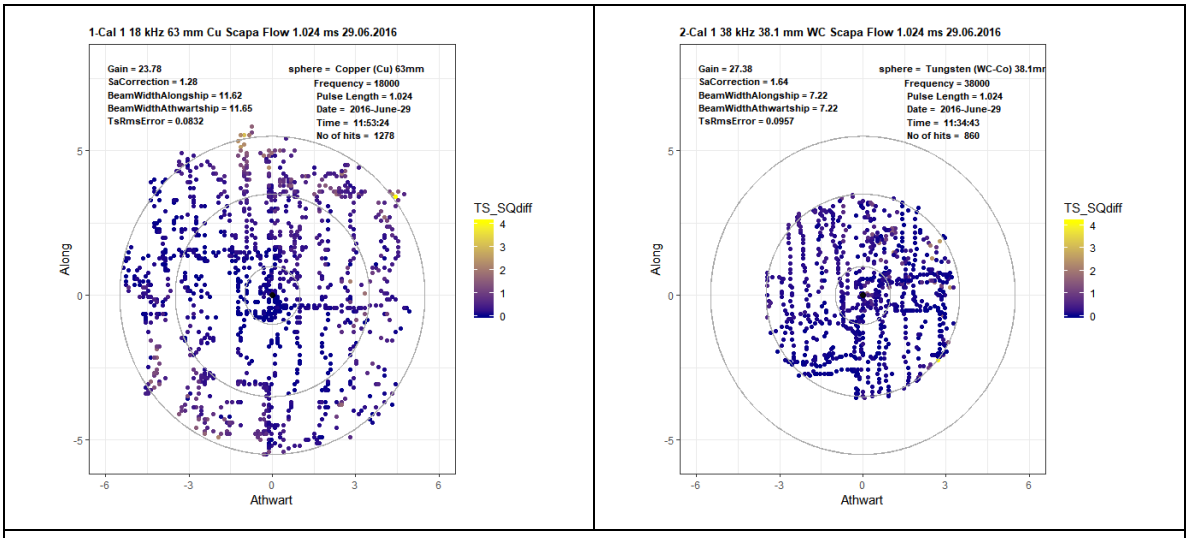

Figure I.5: *Calibration March 2017 Lands End (IBWSS) beam coverage and TS deviation for each target hit at different frequencies.*

I.6 Calibration March-April 2016 Little loch broom

Table I.6: *Calibration Results*

parameter	ES18-11	ES38B	ES70-7C	ES120-7C
Frequency	18000	38000	70000	120000
Gain	23.87	27.54	28.25	27.50
SaCorrection	-0.02	0.01	0.00	-0.01
BeamWidthAlongship	11.52	7.18	6.65	6.56
BeamWidthAthwartship	11.49	7.10	6.64	6.53
TsRms	0.0713	0.0424	0.0364	0.0323
Pulse Length	1.024	1.024	1.024	1.024
Software	1.8.3.0	1.8.3.0	1.8.3.0	1.8.3.0
Firmware	1.70	1.70	1.70	1.70
Date	2016-April-02	2016-April-02	2016-April-02	2016-April-02
Time	06:33:09	06:57:40	07:30:00	10:48:08
No of hits	2333	1638	2076	2102
Sphere	Copper (Cu) 63mm	Tungsten (WC-Co) 38.1mm	Tungsten (WC-Co) 38.1mm	Tungsten (WC-Co) 38.1mm

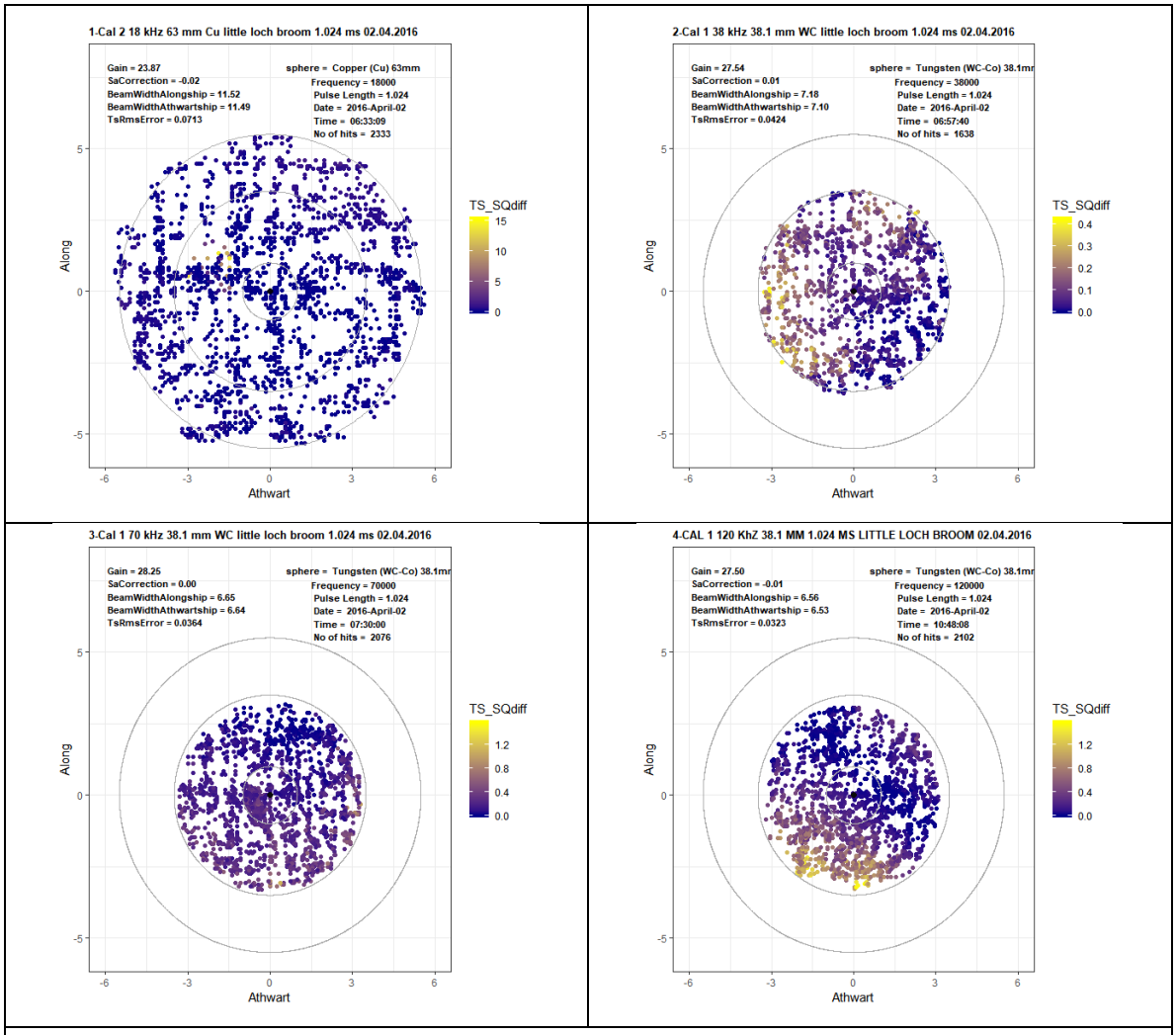

Figure I.6: *Calibration March 2017 Lands End (IBWSS) beam coverage and TS deviation for each target hit at different frequencies.*

I.7 Calibration Feb 2016 Norway

Table I.7: *Calibration Results*

parameter	ES38B	ES70-7C	ES120-7C	ES333-7C
Frequency	38000	70000	120000	333000
Gain	27.43	28.44	27.65	24.78
SaCorrection	-0.01	-0.02	-0.04	-0.13
BeamWidthAlongship	7.16	6.60	6.56	6.50
BeamWidthAthwartship	7.09	6.70	6.44	6.39
TsRms	0.0378	0.0581	0.0710	0.7030
Pulse Length	1.024	1.024	1.024	1.024
Software	1.8.2.0	1.8.3.0	1.8.3.0	1.8.3.0
Firmware	1.70	1.70	1.70	TransceiverSWVersionYetUnknown
Date	2016-February-25	2016-February-26	2016-February-26	2016-February-26
Time	22:23:48	16:26:45	17:30:44	14:29:17
No of hits	1092	426	632	786
Sphere	Tungsten (WC-Co) 38.1mm	Tungsten (WC-Co) 38.1mm	Tungsten (WC-Co) 38.1mm	Tungsten (WC-Co) 22mm

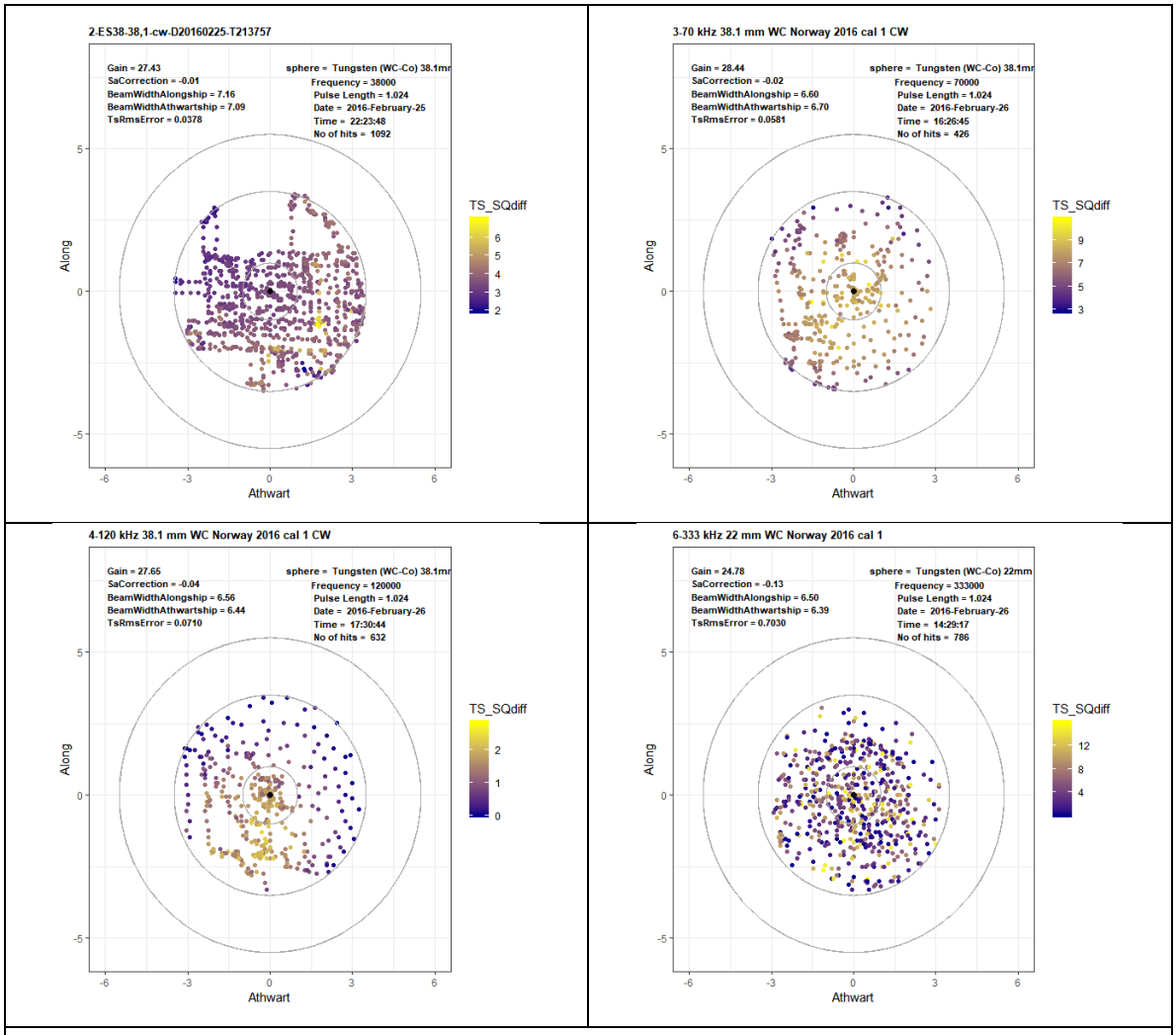

Figure I.7: *Calibration 2016 in Norway. Beam coverage and TS deviation for each target hit at different frequencies.*

I.8 Time Series Plots of EK60 and EK80 calibration parameters

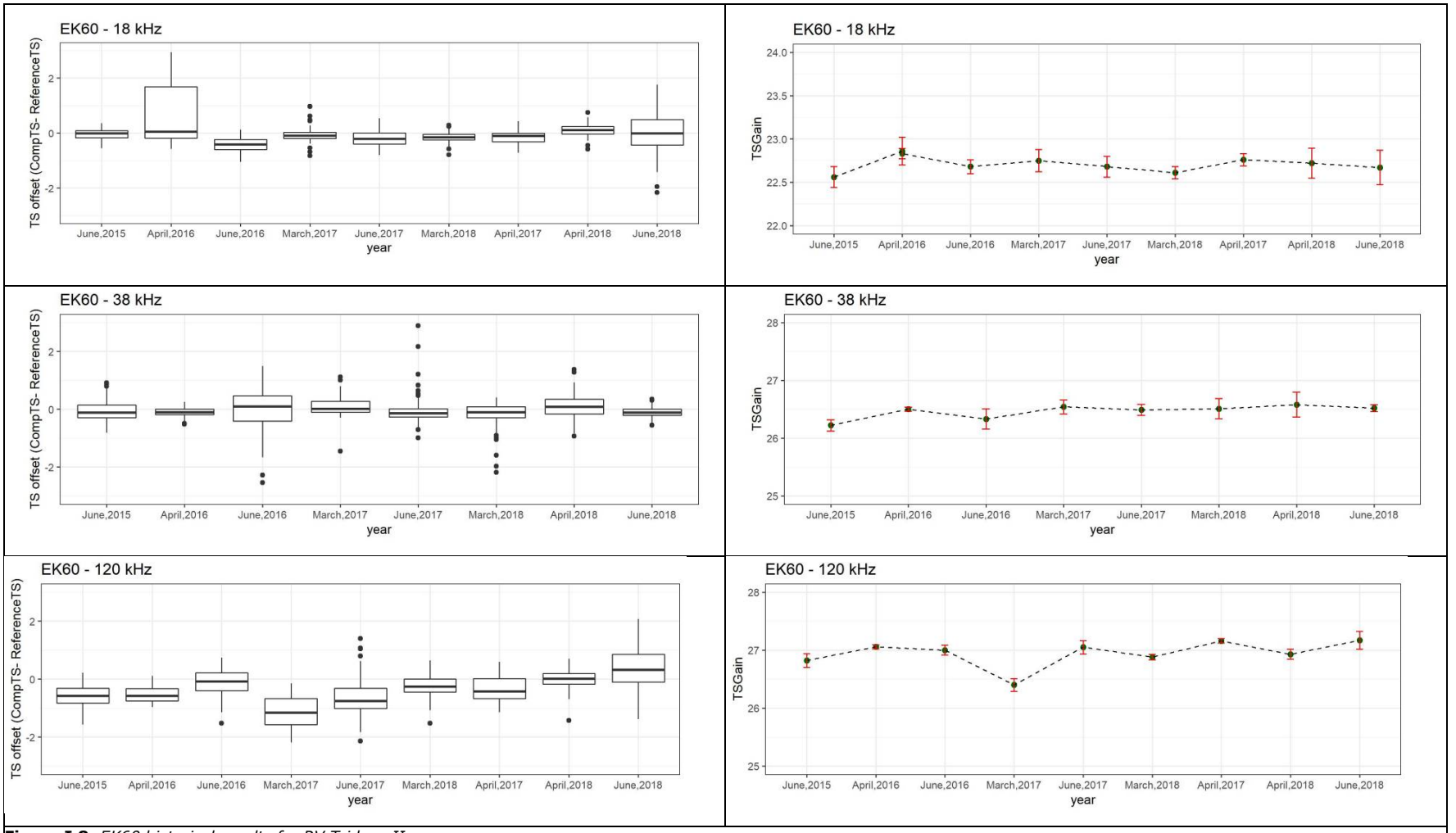

Figure I.8: *EK60 historical results for RV Tridens II.*

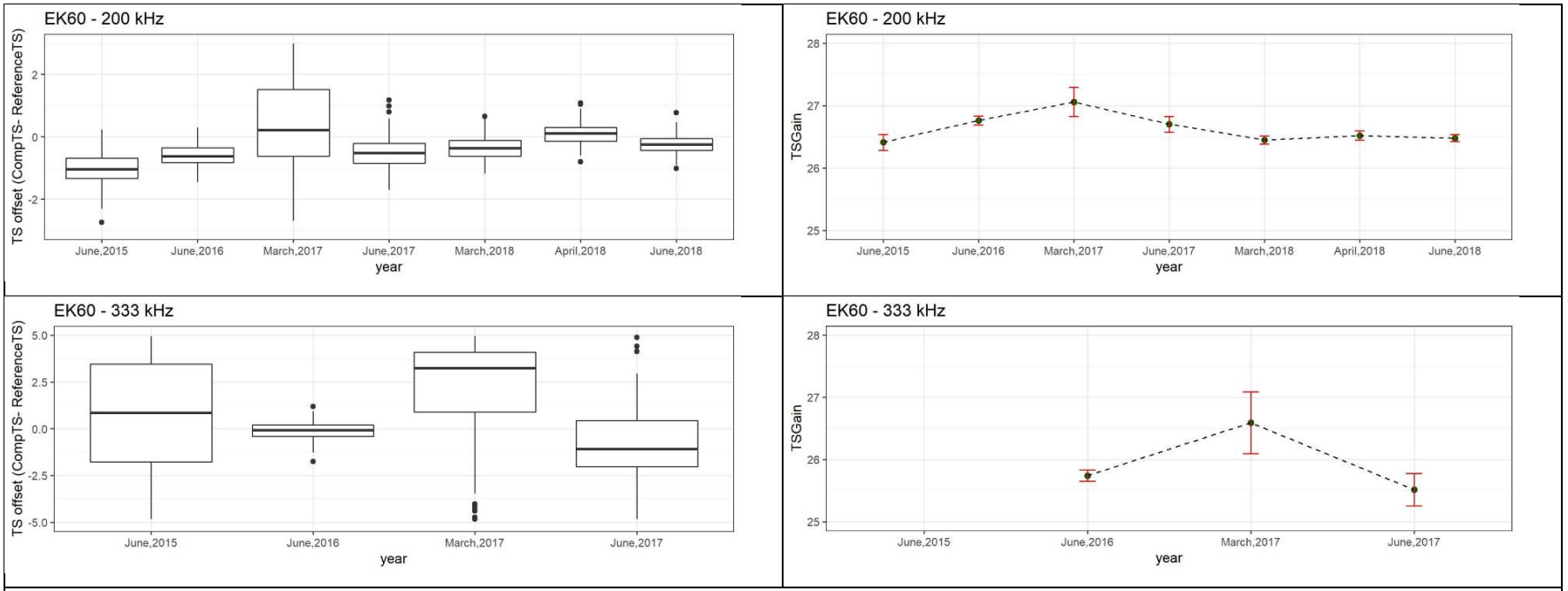

Figure I.8 (continued): *EK60 historical results for RV Tridens II.*

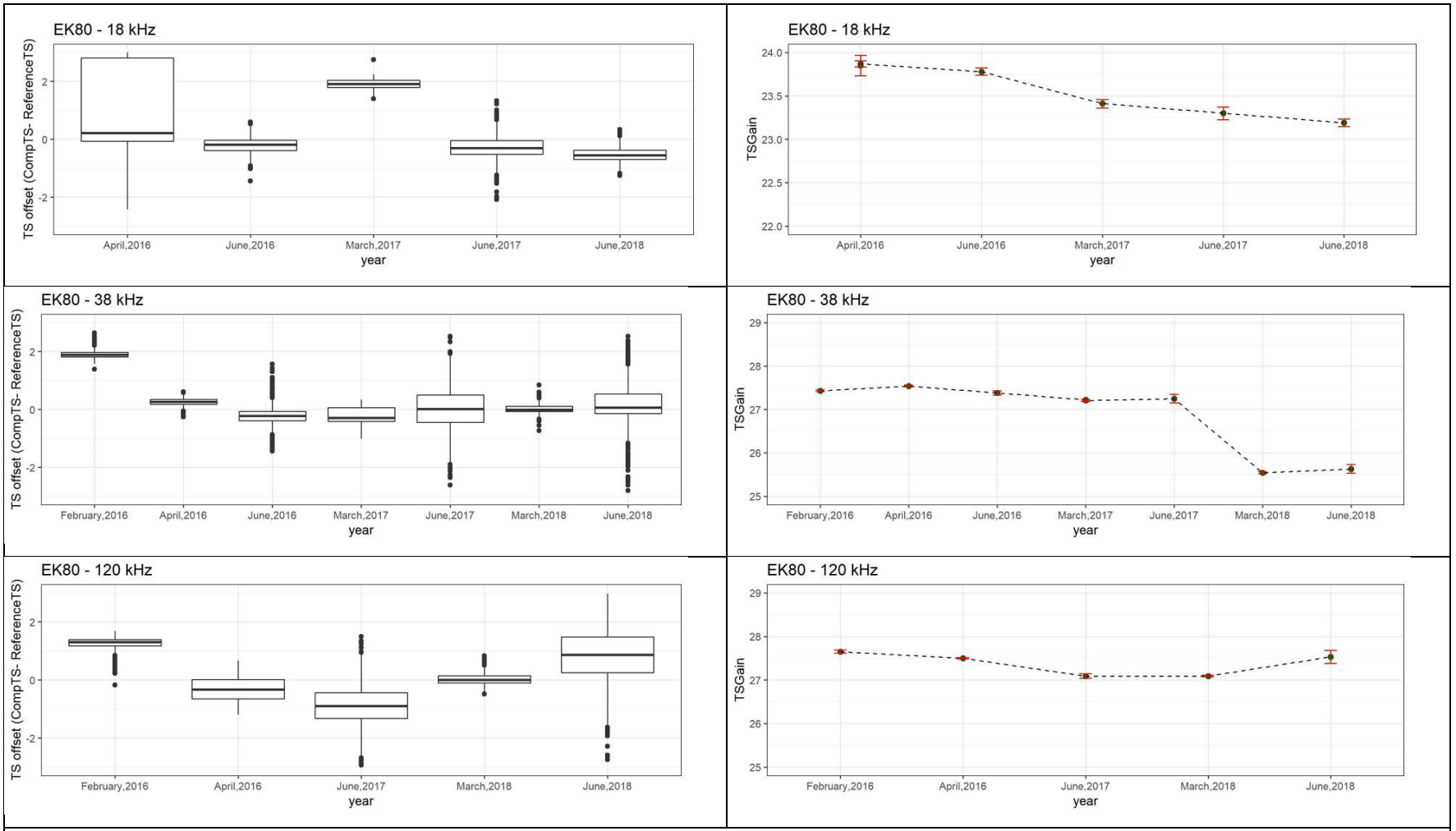

Figure I.9: *EK80 CW historical results for RV Tridens II.*

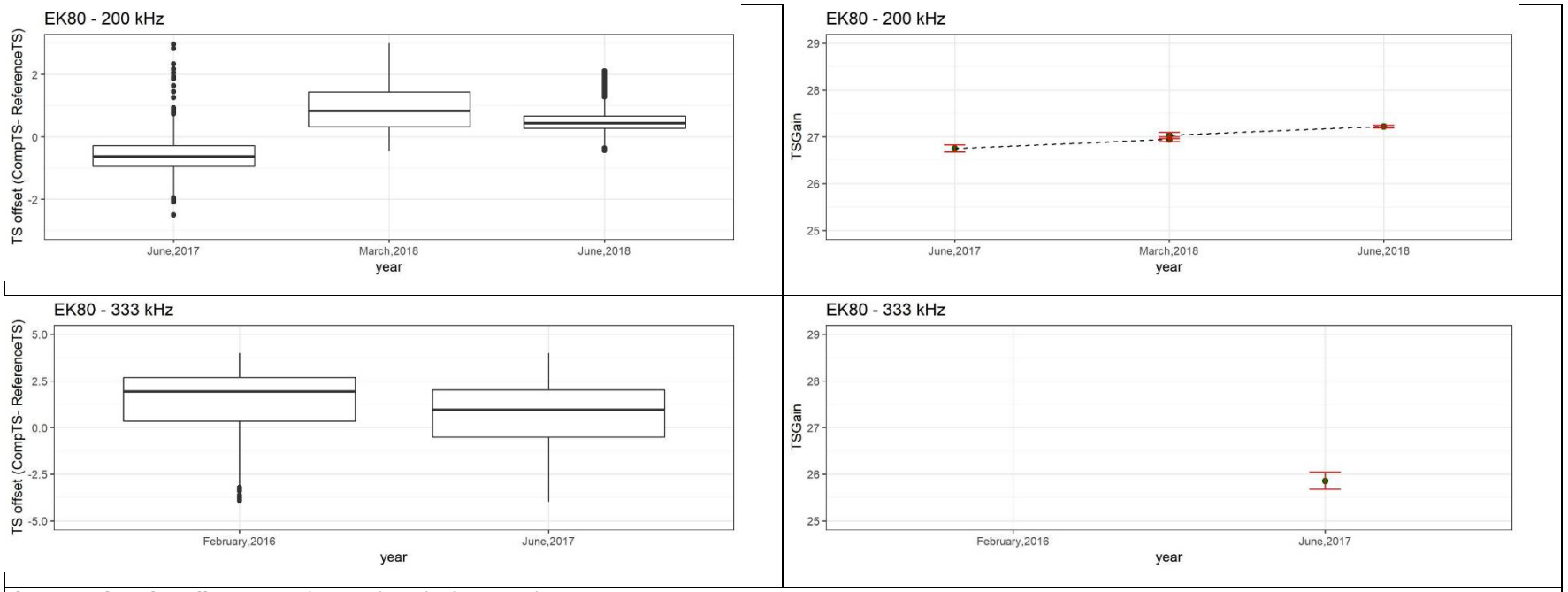

Figure I.9 (continued): *EK80 CW historical results for RV Tridens II.*